

S-24-57

Authority -

DECLASSIFIED- US: 1683

TAINE TO ROBERTSON MEMO

DATED 9/28/66

NACA

Declassified by authority of NASA  
Classification Change Notices No. 10  
Dated \*\* 10/2/64 \*\*

## RESEARCH MEMORANDUM

ALTITUDE PERFORMANCE OF A TURBOJET ENGINE

USING PENTABORANE FUEL

By Joseph N. Sivo

Lewis Flight Propulsion Laboratory  
Cleveland, Ohio

GPO PRICE \$ \_\_\_\_\_

FACILITY FORM 602

N66 39618

(ACCESSION NUMBER)

CFSTI PRICE(S) \$ \_\_\_\_\_

(THRU)

47

(CODE)

Hard copy (HC) \$ 2.00

(NASA CR OR TMX OR AD NUMBER)

125

(CATEGORY)

Microfiche (MF) \$ .50

R 653 JUL 66

NATIONAL ADVISORY COMMITTEE  
FOR AERONAUTICS

WASHINGTON

May 20, 1957

66-48152-8

NACA RM E57C20

DECLASSIFIED

## NATIONAL ADVISORY COMMITTEE FOR AERONAUTICS

Declassified by authority of NASA  
RESEARCH MEMORANDUM Classification Change Notices No. 80  
Dated \*\*-10/10/66

4384  
CO-1  
ALTITUDE PERFORMANCE OF A TURBOJET ENGINE USING PENTABORANE FUEL

By Joseph N. Sivo

## SUMMARY

A turbojet engine having a two-stage turbine was operated with pentaborane fuel continuously for 11.5 minutes at a simulated altitude of 55,000 feet at a flight Mach number of 0.8. The engine incorporated an NACA combustor designed specifically for use with pentaborane fuel.

Although the net-thrust specific fuel consumption was initially reduced 32 percent below that obtained with gasoline fuel, the occurrence of a 25-percent loss in net thrust after 8 minutes of operation resulted in a subsequent increase in specific fuel consumption to a value only 11.5 percent lower than that for gasoline. This thrust deficit stemmed almost entirely from a 3-percentage-point loss in turbine efficiency, which in turn reflected itself primarily in an unusually high tailpipe pressure loss. The tailpipe pressure loss and thus the thrust deficit were magnified by the high initial loading of the turbine and the consequent high exit Mach numbers. With a more conservatively designed turbine the tailpipe losses would be reduced to a fraction of the increased values. An equilibrium condition between the deposition and erosion of boric oxide within the engine was approached after approximately 4 minutes of operation with pentaborane fuel but was not completely established at the end of the run.

## INTRODUCTION

The continuing requirements for increased range and altitude for military aircraft have created considerable interest in the use of high-energy fuel. One group of such fuels currently being considered is the boron hydride family and fuels related to this group. The principal boron hydride that has been used experimentally to date is pentaborane, which has a heating value of 29,000 Btu per pound. A related fuel of interest is ethyldecaborane, which has a heating value of approximately 26,000 Btu per pound.

Pentaborane was considered typical of the boron hydride family insofar as combustion characteristics and products of combustion are concerned and thus was made available in small quantities for combustor and

full-scale engine tests. Initial full-scale turbojet engine tests using pentaborane fuel are reported in references 1 and 2. The results indicated that a significant reduction in engine performance occurred because of boric oxide deposits in the turbine and tailpipe. The turbojet engines used incorporated conventional hydrocarbon-fuel combustors for use with pentaborane fuel. One of the principal reasons for engine performance loss was believed to be runoff of boric oxide from the combustor walls onto the turbine assembly, which resulted in turbine performance losses. It should be noted that the engines of references 1 and 2 incorporated single-stage turbines.

In an effort to minimize the boric oxide runoff from the combustor walls, investigations were conducted in combustor test rigs to determine a combustor design suitable for use with pentaborane fuel. The performance of pentaborane fuel in a quarter-sector annular combustor designed specifically to reduce boric oxide runoff is reported in reference 3.

The primary objectives of the investigation reported herein were to determine the effect of this new combustor design on boric oxide deposition on engine parts and to determine the effect of boric oxide deposition on the performance of a multistage turbine. Therefore, a combustor similar to the combustor of reference 3 was installed in a turbojet engine that incorporated a two-stage turbine. The multistage-turbine engine was selected because it is somewhat representative of the engines presently in use and in the development stage.

Pentaborane fuel (approx. 130 lb) was used in the engine performance evaluation reported herein. The engine was operated in an altitude test chamber of the NACA Lewis laboratory at a simulated altitude of 55,000 feet and a flight Mach number of 0.8. The quantity of pentaborane that was allotted for this investigation permitted 11.5 minutes of continuous engine operation. The data presented herein show the engine component and over-all performance deterioration with operation on pentaborane fuel. Photographs of oxide deposits on the major engine components are also included.

#### APPARATUS

##### Engine

A schematic diagram of the engine used in this investigation is shown in figure 1. The engine consisted of an axial-flow compressor with a moderate pressure ratio, an annular combustor, and a two-stage turbine. An afterburner tailpipe was used with a variable-area clamshell exhaust nozzle which permitted operation at the maximum allowable turbine-outlet gas temperature of  $1170^{\circ}$  F and rated engine speed.

## Combustor

A cross section of the NACA combustor designed for use with pentaborane fuel that was used in this investigation is shown in figure 2. A photograph of the combustor installed in the engine is shown in figure 3; one-half of the outer wall was removed for this photograph. The liner walls were a series of louvers arranged to produce a continuous film of air on the liner walls to minimize the oxide deposition on the walls. A perforated plate was used at the combustor inlet to prevent a recirculation zone in the region of the fuel nozzles. Secondary-mixing air slots were located midway between the fuel nozzles and the combustor exit to control the combustor-outlet temperature profiles. The combustor was geometrically similar to the combustor reported in reference 3.

Details of the air-atomizing fuel nozzles are shown in figure 4. Forty fuel nozzles were used and were equally spaced circumferentially. Twenty of these nozzles were used during pentaborane operation and twenty alternate nozzles were used during operation with gasoline. The nozzles injected radially into the combustor to minimize the area of fuel nozzle exposed to compressor-discharge air temperatures so that fuel heating within the fuel nozzle would be minimized. The air used for atomization also provided cooling.

## Fuel System

A dual fuel system was used which allowed operation with either pentaborane or gasoline fuel. In the pentaborane fuel system helium pressure was used to force pentaborane fuel into the engine. A diagram of the pentaborane fuel system is shown in figure 5. The purge system used helium and dry JP-4 fuel alternately to inert the system before and after the pentaborane fuel test. The standard engine fuel system was used for the gasoline fuel.

## Fuel Properties

The gasoline used was 72-octane unleaded fuel with a lower heating value of 18,850 Btu per pound. The pentaborane used had a purity of approximately 99 percent, and its properties were as follows:

Molecular weight . . . . .	63.17
Melting point, °F . . . . .	-52
Boiling point at 760 mm Hg, °F . . . . .	136
Lower heat of combustion, Btu/lb . . . . .	29,100
Specific gravity at 32° F . . . . .	0.644
Stoichiometric fuel-air ratio . . . . .	0.0764
Pounds of B <sub>2</sub> O <sub>3</sub> per million Btu . . . . .	94

### Instrumentation

Location of instrumentation stations and the number of pressure and temperature instruments at each station are shown in figure 1. Engine airflow was measured at station 1. The fuel flow was measured with vane-type flowmeters in both fuel systems. Engine jet thrust was measured with a null-type thrust cell.

### Installation

The engine was installed in an altitude test chamber which consists of a tank 10 feet in diameter and 60 feet long divided into two compartments by a bulkhead. Air at ram pressure was ducted from the front compartment to the engine inlet through a bellmouth inlet and a Venturi, which was used to measure airflow. A labyrinth seal around the inlet duct was used to prevent leakage from the front to the rear compartment where the ambient altitude pressure was maintained. The engine was mounted on a thrust-measuring platform in the rear compartment.

### PROCEDURE

The engine operating conditions, established during operation on gasoline fuel, simulated a pressure altitude of 55,000 feet at a flight Mach number of 0.8 with an engine-inlet temperature of 60° F. The engine was operated at rated speed with an exhaust-gas temperature of 1170° F. At this test point engine performance data were recorded. The pentaborane fuel system was then purged with both helium and dry JP-4 fuel to eliminate air and any contamination in the fuel system. Following the system purge the pentaborane supply tank was pressurized with helium. With the engine operating at the aforementioned test conditions, a switch in fuels was made by gradually decreasing the gasoline flow and increasing pentaborane flow until the engine was operating solely on pentaborane. The switchover was accomplished in approximately 45 seconds. During operation with pentaborane exhaust-nozzle area and engine fuel flow were modulated to hold engine speed and exhaust-gas temperature constant at their initial values. When the exhaust nozzle was fully open, engine fuel flow and speed were reduced so as to maintain the exhaust-gas temperature approximately constant.

The duration of the run with pentaborane was 11.5 minutes. Data were taken at approximately 30-second intervals during the run. The data taken are presented in table I. The symbols used herein are listed in appendix A and the methods of calculation are presented in appendix B.

## RESULTS AND DISCUSSION

## Oxide Formation and Deposition

One of the products of combustion of boron compounds is boric oxide, which is a viscous fluid at the temperatures generally encountered in turbojet engines. If thermal decomposition of pentaborane fuel occurs, the decomposed fuel forms clinkers similar to the coke from hydrocarbon fuels. The amount of fuel consumed during the 11.5 minutes of operation with pentaborane resulted in formation of about 356 pounds of boric oxide. The major portion of this oxide passed through the engine in the form of microscopic drops of liquid suspended in the main gas stream. However, significant amounts were deposited on the metal surfaces in the hot sections of the engine. The weight of the oxide deposited on engine parts was not determined.

Examination of the combustor section following the run showed that the majority of the pentaborane fuel nozzles were relatively free of oxide deposits. However, the fuel nozzles adjacent to the combustor split line had large clinker formations (decomposed fuel) surrounding the nozzle as shown in figure 6. The turbine stator immediately downstream of these clinker formations had chunks of clinker wedged in the stator passages. (The two fuel nozzles missing in the photograph of fig. 6(b) were removed during a preliminary inspection of the engine.) The combustor walls were generally free of heavy oxide deposits, and the condition of the combustor indicated that oxide runoff from the walls was a minimum. A sketch of the oxide deposit that occurred is shown in figure 6(c).

The oxide deposits that occurred on the first-stage turbine stator (fig. 7(a)) were fairly uniform in thickness from root to tip with the exception of clinkers previously mentioned. The blade surfaces were roughened by the buildup of oxide and by bits of decomposed fuel embedded in the oxide. The effect that shutting down the engine had on these deposits could not be determined. It is possible that during the engine shutdown, the oxide-film roughness increased because of the reduction in temperatures. The first-stage rotor blade surfaces (fig. 7(b)) were relatively free of oxide; however, there were indications (fine radial ridges) of radial flow of oxide from root to tip on the blades. These ridges roughened the surfaces of the blades. The leading edges of the second-stage stator blades (fig. 7(c)) were relatively free of oxide deposits, although oxide deposits in the blade passages and at the trailing edges were heavy, as shown in figure 7(d). It can be seen that oxide deposition was greater on the suction surfaces of the blades. As a result of the centrifuging action of the first-stage rotor, the oxide deposits on the second-stage stator were heavier at the blade tip than at the blade root. Some partial blocking of the stator passages occurred in the tip sections of the blades. The second-stage turbine rotor blades

(fig. 7(e)) like the first-stage rotor blades indicated a radial flow of oxide on the blades. There was a slight buildup of oxide at the blade tips. It could not be determined whether this buildup occurred during engine shutdown. Both sets of turbine rotor blades showed evidence of rubbing at the tips in the oxide deposits present on the shrouds. Inspection of the blade tips indicated that the rubbing occurred with engine windmilling after the run when the oxide was actually a solid.

The tailpipe diffuser section (fig. 8(a)) had relatively heavy oxide deposits ranging from  $1/8$  to  $1/4$  inch thick. The heavy deposit covered a length of approximately 2 feet on the outer cone and 1.5 feet on the inner cone. Downstream of the heavy deposits the surfaces of the tailpipe and tailcone were coated with a very thin film of boric oxide (fig. 8(b)). The tailpipe skin temperature was approximately  $1100^{\circ}$  F. The deposit that occurred at the exhaust-nozzle rim (fig. 8(b)) appeared to be a mixture of boric oxide in the vitreous and crystalline states and was not great enough to interfere with nozzle operation or greatly decrease nozzle area.

#### Engine Operating Point

The accumulation of boric oxide deposits on the metal surfaces of the engine resulted in decreases in the performance of the turbine and the tailpipe. In order to evaluate these performance decreases it was necessary to maintain the test point throughout the run with pentaborane. The exhaust-gas temperature (fig. 9(a)) was held within  $\pm 10^{\circ}$  of the selected test point temperature of  $1170^{\circ}$  F. To compensate for the decreases in turbine and tailpipe performance it was necessary to increase the exhaust-nozzle area to maintain this temperature level. The exhaust-nozzle area (fig. 9(b)) was increased rapidly during the early portion of the run. The fully open nozzle position was reached after 4 minutes of operation. During this time interval the nozzle area was increased to 130 percent of rated nozzle area. Engine speed (fig. 9(c)) was held essentially constant at rated corrected engine speed for the first 8 minutes of operation. However, since the exhaust nozzle was fully open the exhaust-gas temperature increased gradually during the second 4 minutes, and it was necessary at the end of 8 minutes to decrease engine speed in order to avoid excessive overtemperature of the engine.

#### Effect of Oxide Deposits on Component Performance

The combustion efficiency (fig. 10(a)) obtained with pentaborane fuel at the beginning of the run was 95 percent and was equal to the efficiency obtained with gasoline fuel. Efficiency decreased from 95 to 92 percent during the run. The drop in efficiency was probably due to the malfunctioning of some fuel nozzles, which caused partial decomposition of some of the fuel. This is evidenced by clinker formations present in

the combustor. The combustor total-pressure loss (fig. 10(b)) remained constant at 0.053 throughout the run except during the speed reduction at the end of the run where the loss decreased slightly.

The turbine efficiency (fig. 11(a)) decreased from 82 to 79 percent during the first 4 minutes of the run. The initial efficiency level was about the same as that obtained with gasoline. The efficiency decrease after the first 4 minutes was less than 1 percent. As was mentioned previously, the turbine stators had an accumulation of boric oxide on the blade surfaces. This oxide accumulation resulted in a decrease in the stator effective flow areas. The decrease in the first-stage stator area during the run is shown in figure 11(b). The stator flow area was calculated assuming choked flow in the stator passage. The total decrease in area was 4.7 percent, the greatest rate of area change occurring during the early portion of the run. This decrease in stator area required an increase in compressor pressure ratio to maintain flow and thus an increase in compressor work. The increase in work manifested itself as the increase in turbine total-temperature ratio shown in figure 11(c). The effect of this increase in work was small, however, and resulted in only a  $15^{\circ}$  R increase in turbine-inlet temperature. Since the change in turbine stator area after 4 minutes was relatively small, its effect on turbine temperature ratio was not discernible. As a result of the decrease in turbine efficiency, the increase in compressor work, and the change in the thermodynamic properties of the combustion products of pentaborane fuel as compared with gasoline fuel, the turbine total-pressure ratio (fig. 11(d)) was necessarily increased over the pressure ratio required for operation with gasoline fuel. The pressure ratio increased rapidly during the first 4 minutes and then was essentially constant at a ratio 13 percent higher than the initial value.

A comparison of the turbine-efficiency decrease for the engine reported herein and that of the single-stage-turbine engine of reference 2 is shown in figure 12. Generally speaking, the magnitude of efficiency decrease in both cases is similar. However, the curves indicate that the rate of efficiency decrease early in the run was higher with the two-stage turbine of this investigation.

The decrease in turbine performance and the change in thermodynamic properties of combustion products of pentaborane both result in increased turbine-outlet Mach numbers. Turbine-outlet Mach number plotted against time is shown in figure 13. Also included is a curve showing the Mach number variations for the data of reference 2. The turbine-outlet Mach number for the engine reported herein is initially 0.69 but increases rapidly to a value of 0.95 at the end of 4 minutes and then remains at this value until speed reduction causes a small reduction in Mach number at the end of the run. Although the change in turbine performance and the change in gas properties were similar in the investigation reported herein and in that of reference 2, the changes in turbine-outlet Mach

number were greatly different. This difference results primarily from the extremely high initial turbine-outlet Mach number of the engine used in this investigation (0.69) as compared to the value for the engine of reference 2 (0.49). As this initial Mach number level increases, a given percentage change in turbine efficiency will have a disproportionately greater effect on the final Mach number and consequently on the pressure losses in the tailpipe.

The tailpipe total-pressure loss, which includes diffuser losses, is presented in figure 14(a) for the tailpipe used in this investigation. The pressure loss increased rapidly from 6.5 to 21 percent during the first 4 minutes of operation and was constant thereafter. The variation in pressure loss resulted primarily from the increase in turbine-outlet Mach number mentioned previously and from an increase in tailpipe drag coefficient due to oxide deposition. 4384

To separate the effects of tailpipe Mach number and drag coefficient, the tailpipe pressure loss is presented in figure 14(b) as a function of tailpipe-inlet Mach number, that is, turbine-outlet Mach number for both the gasoline and pentaborane fuel runs. The Mach numbers presented are based on the turbine-outlet area of the clean pipe. The curve for gasoline was obtained by variation of engine speed and exhaust-nozzle area. The separation of the two curves is believed principally due to changes in drag coefficient and changes in flow coefficient or effective flow area in the pipe due to the presence of oxide particles on the walls and in the gas stream. A change in tailpipe drag coefficient would be expected to be more pronounced as the Mach number level increases. The contributions of the flow coefficient and the drag coefficient could not be determined.

A comparison of the tailpipe pressure loss of this investigation with the loss encountered in reference 2 is shown in figure 15. Curves for both hydrocarbon fuel and pentaborane fuel are shown for each engine. The difference in slopes of the pressure-loss curves of the two engines is due to differences in inlet flow conditions for the two pipes such as whirl and tailpipe configuration. Again it is illustrated that low turbine-outlet Mach numbers are necessary to minimize tailpipe total-pressure losses.

#### Effect of Oxide Deposition on Over-All Performance

The decrease in turbine and tailpipe performance was reflected in a decrease in engine total-pressure ratio at constant engine temperature ratio. The effect of component performance deterioration on engine pressure ratio is presented in figure 16. The engine pressure ratio decreased rapidly from 1.87 to 1.45 during the first 4 minutes of operation. Engine pressure ratio approached an equilibrium at the end of 4 minutes of operation. The decrease after 8 minutes resulted primarily from the

decrease in engine speed. Although the performance decrease after 4 minutes was at a reduced rate, an equilibrium condition was not reached by the end of the run.

The over-all net thrust of the engine is presented in figure 17 as a percent of the thrust obtained with gasoline at the same operating point. There is an initial decrease in net thrust of approximately 6 percent at zero time. This initial drop in thrust is due to the effect of the change in the gas properties of pentaborane as compared with gasoline on the performance of the turbine and tailpipe. Thrust continued to drop with pentaborane operation, a loss in thrust of 25 percent having occurred by the end of 4 minutes. The thrust was essentially constant during the second 4 minutes. The loss in thrust from 8 minutes to the end of the run was primarily due to engine speed reduction.

The variation in net-thrust specific fuel consumption in percent of the specific fuel consumption obtained with gasoline fuel is shown in figure 18. The initial decrease in fuel consumption was 32 percent, which is within 1 percent of the decrease expected. However, primarily as a result of the net-thrust loss, the specific fuel consumption increased rapidly during the first 4 minutes of operation and at the end of 8 minutes was only 11.5 percent lower than with gasoline fuel.

A breakdown of the factors contributing to the thrust losses is presented in figure 19. These data also reflect the deficit occurring in specific fuel consumption. Of the initial 6-percent loss in thrust mentioned previously, the change in thermodynamic properties of the combustion products results in a 4.5-percent loss in thrust based on the gas conditions at the turbine outlet. This includes a 0.6-percent loss resulting from the mass-flow decrease caused by the lower fuel flows accompanying the higher heating value of pentaborane fuel. This initial loss is inherent with pentaborane fuel. The reduction of 0.03 in turbine efficiency produced a direct thrust loss of 5 percent. The effect of the turbine-efficiency deficit is further reflected in the increased tailpipe total-pressure loss which accounted for an additional 15-percent thrust loss.

It is immediately obvious that large thrust and specific-fuel-consumption improvements could be realized if no turbine-efficiency reduction occurred. The principal gain would come from reduced tailpipe losses, which are primarily a result of increased turbine-outlet Mach numbers that accompany the turbine-efficiency deterioration. Therefore, in this particular case, improvements in turbine efficiency would indirectly result in major improvements in the engine net thrust and specific fuel consumption. The effect of turbine performance changes on turbine-outlet Mach number can be minimized by the use of turbines that have low turbine-outlet Mach numbers.

## Operational Comments

In order to obtain an engine operating reference point at the test altitude and to conserve pentaborane fuel, it was necessary to operate the engine on a hydrocarbon fuel. An attempt was made to use JP-4 as the reference-point fuel. Although the engine combustor operated with this fuel, considerable torching through the turbine occurred. To minimize this torching a more volatile fuel was needed. A 72-octane gasoline was selected and proved to be a satisfactory fuel for use in the special combustor.

## SUMMARY OF RESULTS

A turbojet engine incorporating an NACA combustor designed specifically for use with pentaborane fuel was operated continuously for 11.5 minutes on pentaborane fuel. The engine also had a two-stage turbine in contrast to single-stage turbines used in all the previously reported full-scale engine investigations with pentaborane fuel. Initially there was a 32-percent reduction in specific fuel consumption over that obtained with gasoline fuel. However, after 8 minutes of operation the net-thrust specific fuel consumption was only 11.5 percent lower than for gasoline. The occurrence of a 25-percent loss in net thrust after 8 minutes of operation plus a reduction in combustion efficiency resulted in this increase in specific fuel consumption.

A major portion of the thrust loss was a result of a reduction in turbine efficiency. The loss in turbine performance was relatively small; the maximum reduction in efficiency was only 3 percent. However, since the initial outlet Mach number of this turbine was high, the small reduction in turbine efficiency greatly increased the turbine-outlet Mach number. These high Mach numbers resulted in unusually high tailpipe pressure losses and thus thrust losses. The use of a more lightly loaded turbine with correspondingly lower outlet Mach numbers would greatly improve the over-all engine performance.

The low rate of engine performance deterioration after approximately 4 minutes of operation, indicated an approach to an equilibrium condition between the deposition and erosion of boric oxide on engine parts. However, the performance deterioration was continuing at a reduced rate at the end of the run. Since the run was only 11.5 minutes in length, it is difficult to predict from the data obtained in this test the result of prolonged operation with pentaborane fuel.

Lewis Flight Propulsion Laboratory  
National Advisory Committee for Aeronautics  
Cleveland, Ohio, March 21, 1957

~~DECLASSIFIED~~

## APPENDIX A

## SYMBOLS

The following symbols are used in this report:

- A area, sq ft  
F<sub>j</sub> jet thrust, lb  
F<sub>n</sub> net thrust, lb  
F<sub>s</sub> thrust system scale reading, lb  
g acceleration due to gravity, ft/sec<sup>2</sup>  
P total pressure, lb/sq ft  
p static pressure, lb/sq ft  
R gas constant, ft-lb/(lb)(°R)  
T total temperature, °R  
V velocity, ft/sec  
w weight flow, lb/sec  
γ ratio of specific heats  
η efficiency

## Subscripts:

- a airflow  
at atomizing  
B combustor  
Cl compressor seal leakage  
cc camera cooling  
f fuel  
i vena contracta at exhaust-nozzle outlet

s scale  
sl seal  
T turbine  
Tf turbine flange  
t total weight flow  
0 free stream  
1 airflow measuring station  
2 compressor inlet  
3 compressor outlet  
4 turbine inlet  
5 turbine outlet  
9 exhaust-nozzle inlet  
10 exhaust-nozzle discharge

REF ID: A6472  
DECLASSIFIED

## APPENDIX B

## METHODS OF CALCULATION

## Airflow

Engine-inlet airflow was calculated from measurements at station 1 by use of the following equation:

$$w_{a,1} = C_{fl} A_1 p_1 \sqrt{\frac{g}{RT_1}} \sqrt{\frac{2\gamma_1}{\gamma_1 - 1} \left(\frac{P}{p}\right)} \left[ \frac{\gamma_1 - 1}{\gamma_1} \left[ \left(\frac{P}{p}\right) - 1 \right] \right]$$

A flow coefficient  $C_{fl}$  of 0.994 was used and is defined as the ratio of the actual flow to the airflow computed on the basis of one-dimensional flow by use of free-stream total pressures and the static pressure in the Venturi throat.

Compressor-leakage, turbine-flange-cooling, atomizing-air, and camera-cooling airflows were calculated from total pressures, total temperatures, and static pressure in the same manner as engine airflow. The airflows and gas flows at the various stations throughout the engine were calculated as follows:

$$w_{a,2} = w_{a,1}$$

$$w_{a,3} = w_{a,2} - w_{a,Cl} - w_{a,Tf}$$

$$w_{a,4} = w_{a,3} + w_{a,at}$$

$$w_{a,5} = w_{a,4}$$

$$w_{a,9} = w_{a,2} - w_{a,Cl} + w_{a,at} + w_{a,cc}$$

$$w_{t,4} = w_{a,4} + w_f$$

$$w_{t,9} = w_{a,9} + w_f$$

### Thrust

The over-all jet thrust determined from the thrust-system measurements was calculated from the following equation:

$$F_j = F_s + A_{sl}(p_1 - p_{10})$$

where  $A_{sl}$  is the area of the seal around the engine inlet.

The net thrust was determined by subtracting the inlet momentum from the jet thrust:

$$F_n = F_j - \frac{w_{a,1}V_0}{g}$$

The calculated jet thrust used in determining the breakdown of thrust loss was obtained from the following equation:

$$F_{j,5} = \left[ \frac{w_{t,5}}{g} V_i + A_i(p_i - p_0) \right] C_V$$

The calculation was made using the measured values of pressure, temperature, and mass flow at the turbine outlet. A value for the velocity coefficient  $C_V$  of 0.95 was determined for the exhaust nozzle from a ratio of measured jet thrust to calculated jet thrust at the exhaust nozzle.

### Combustion Efficiency

Combustion efficiency is defined as the ratio of ideal engine fuel flow to actual engine fuel flow:

$$\eta_B = \frac{w_{f,id}}{w_{f,act}}$$

The ideal fuel flow is defined as the fuel flow required to satisfy a heat balance across the engine using the measured temperatures and an ideal combustion process. Fuel flows associated with ideal combustion processes were obtained from unpublished data.

### Combustor-Outlet Temperature

A heat balance across the combustor using the ideal engine fuel flow and the combustor-inlet temperature was made to calculate combustor-outlet temperature. The temperature rise associated with an ideal fuel flow was obtained from unpublished data.

### Turbine Efficiency

Turbine efficiency was calculated from the following equation:

$$\eta_T = \frac{1 - \frac{T_5}{T_4}}{\frac{r-1}{r}}$$

$$1 - \left( \frac{P_5}{P_4} \right)^{\frac{1}{r}}$$

4384

### Area

Turbine stator area and exhaust-nozzle area were calculated as follows:

$$A = \frac{w_t \sqrt{\frac{RT}{g}}}{p \sqrt{\frac{2r}{r-1} \left( \frac{P}{p} \right)^{\frac{r-1}{r}} \left[ \left( \frac{P}{p} \right)^{\frac{r-1}{r}} - 1 \right]}}$$

where  $P/p$  is considered critical.

### Turbine-Outlet Mach Number

The turbine-outlet Mach number was calculated using the mass flow, total temperature, total pressure, and area at the turbine outlet.

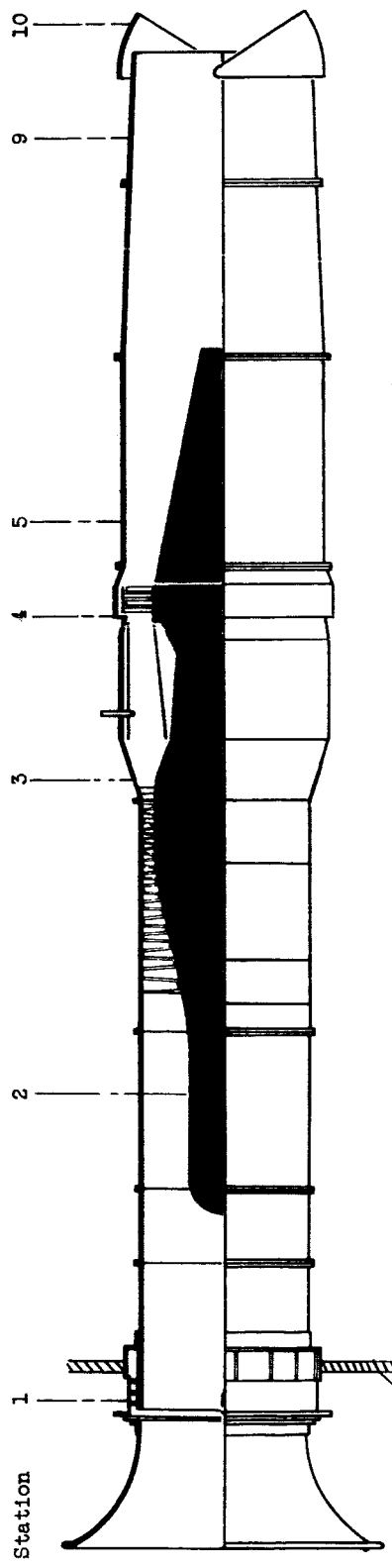
### REFERENCES

1. Useller, James W., Kaufman, Warner B., and Jones, William L.: Altitude Performance of a Full-Scale Turbojet Engine Using Pentaborane Fuels. NACA RM E54K09, 1957.
2. Useller, James W., and Jones, William L.: Extended Operation of Turbojet Engine with Pentaborane. NACA RM E55L29, 1957.
3. Kaufman, Warner B., Lezberg, Erwin A., and Breitwieser, Roland: Preliminary Evaluation of Pentaborane in a 1/4-Sector of an Experimental Annular Combustor. NACA RM E56B13, 1957.

TABLE I. - ENGINE PERFORMANCE DATA  
 [Pentaiorane fuel, except for first three runs;  
 compressor-inlet total temperature, 523° R.]

Operation time, min	Compressor inlet pressure, $P_2$ , lb/sq ft abs	Altitude, ambient pressure, $P_0$ , lb/sq ft abs	Compressor outlet total pressure, $P_3$ , lb/sq ft abs	Compressor outlet total temperature, $T_4$ , °R	Compressor outlet total pressure, $T_5$ , °R	Computed turbine inlet total temperature, $T'_4$ , °R	Turbine outlet total pressure, $P'_5$ , lb/sq ft abs	Exhaust nozzle inlet total pressure, $P_g$ , lb/sq ft abs	Exhaust nozzle inlet total temperature, $T_g$ , °R	Engine speed, rpm	Engine inlet airflow, $w_{a,5}$ , lb/sec	Compressor outlet airflow, $w_{a,5}$ , lb/sec	Exhaust nozzle inlet weight flow, $w_n$ , lb/sec	Engine nozzle inlet weight flow, $w_f$ , lb/hr
(a)	2.61	181	2019	1021	1926	2061	580	544	1632	8250	16.57	16.17	16.39	97.9
(a)	2.61	182	2025	1021	1920	2061	581	547	1632	8291	16.61	16.21	17.03	98.1
(a)	2.61	182	2024	1021	1920	2061	582	545	1634	8308	16.53	16.13	16.95	97.6
0.46	2.62	186	2028	1012	1953	2054	567	521	1624	8127	16.07	15.68	16.05	63.6
0.52	2.62	186	2028	1012	1953	2054	553	485	1632	6254	16.42	16.02	16.39	62.8
1.75	2.64	150	2046	1027	1938	2081	552	450	1634	8279	16.49	16.23	16.47	64.2
2.17	2.64	154	2050	1030	1935	2084	535	470	1624	6307	16.37	15.51	16.35	64.0
2.67	2.64	156	2043	1026	1926	2077	532	464	1628	8272	16.49	16.03	16.47	64.0
3.17	2.64	156	2045	1028	1934	2076	523	452	1624	8260	16.37	16.37	16.35	64.0
3.58	2.64	157	2045	1028	1940	2077	522	431	1624	8278	16.42	16.02	16.40	64.0
4.06	2.60	183	2051	1031	1944	2079	524	407	1624	8286	16.40	16.01	16.38	64.0
4.58	2.60	188	2057	1030	1945	2078	523	410	1626	8292	16.45	16.01	16.38	64.2
5.08	2.60	188	2062	1033	1952	2081	522	414	1626	8284	16.40	16.03	16.37	64.2
5.50	2.60	189	2065	1035	1959	2088	522	415	1632	8307	16.43	16.05	16.40	64.2
6.00	2.60	190	2071	1033	1962	2088	526	418	1634	8258	16.45	16.05	16.43	65.4
6.50	2.60	161	2064	1034	1953	2089	523	418	1632	8302	16.41	16.01	16.38	65.4
7.08	2.60	193	2072	1035	1970	2090	523	417	1632	8295	16.39	15.99	16.36	65.4
7.50	2.62	183	2075	1035	1970	2097	528	418	1638	8254	16.42	16.02	16.39	65.4
8.00	2.62	193	2043	1035	1938	2083	518	414	1624	8245	16.35	15.93	16.30	64.5
8.58	2.64	195	2057	1031	1952	2079	521	414	1626	8255	16.28	15.86	16.25	64.5
9.08	2.64	194	2047	1035	1944	2061	515	412	1626	8229	16.19	15.79	16.16	64.5
9.50	2.60	197	2044	1031	1942	2079	518	411	1624	8224	16.14	15.75	16.12	64.2
10.08	2.61	197	2042	1032	1935	2087	522	412	1630	8226	16.13	15.74	16.11	64.2
10.50	2.60	198	2037	1031	1932	2079	518	407	1624	8200	16.06	15.61	15.97	63.0
11.08	2.60	198	2036	1030	1938	2085	518	404	1628	8217	16.05	15.66	16.03	63.9
11.58	2.61	197	2035	1030	1930	2113	521	407	1663	8250	16.07	15.68	16.05	63.6

a. Not timed (gasoline fuel).



Station	Number of probes		
	Static pressure	Total pressure	Total temperature
1	4	4	-
2	-	10 Individual probes 3 Averaging rakes	8
3	-	15	10
4	-	15	30
5	-	20	35
9	-	24	24
10	4	-	-

Figure 1. - Schematic sketch of engine showing station locations.

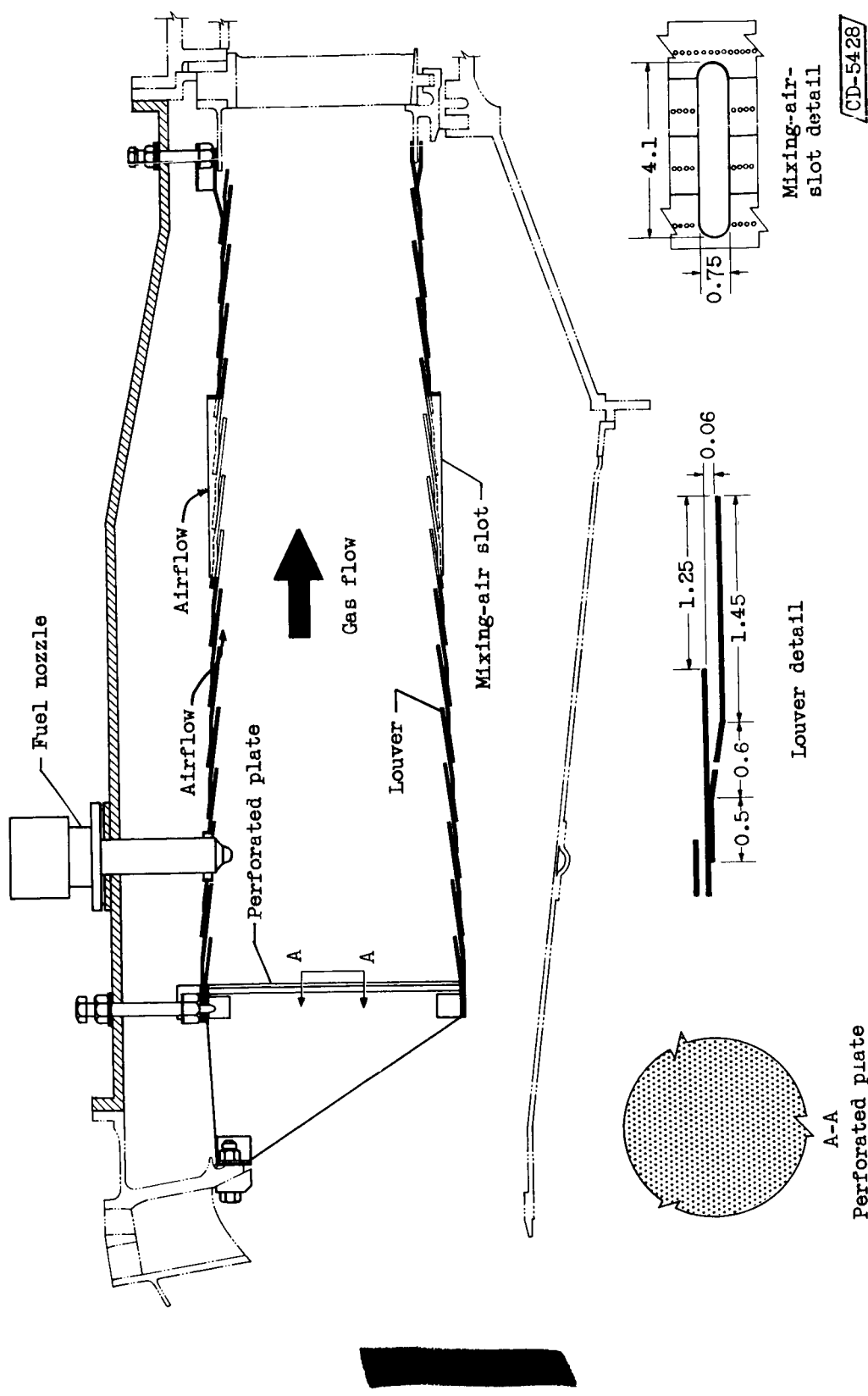


Figure 2. - Cross section of annular combustor. (All dimensions in inches.)

DECOMMISSIONED

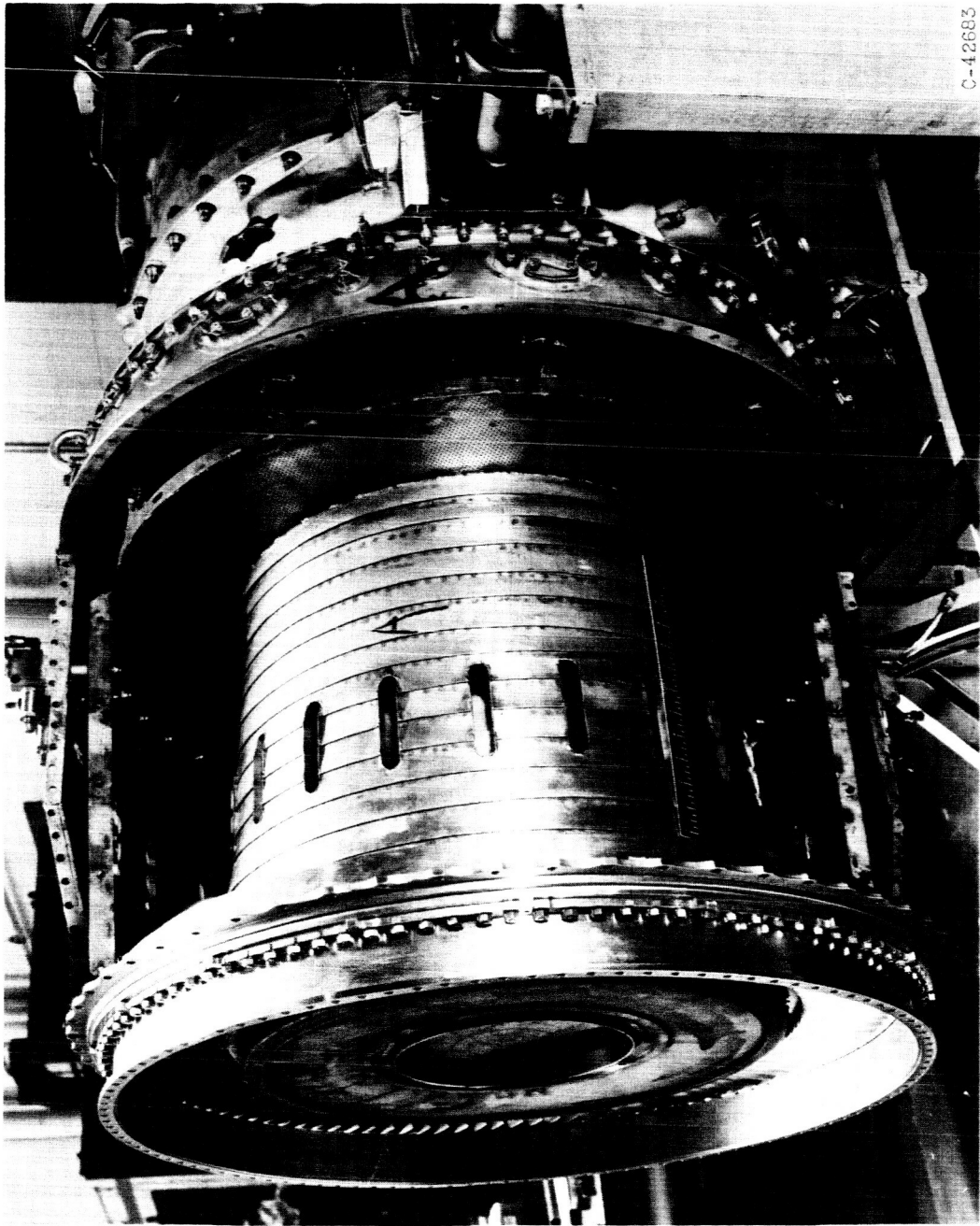


Figure 3. - Annular combustor installed in engine with one-half of outer wall removed.

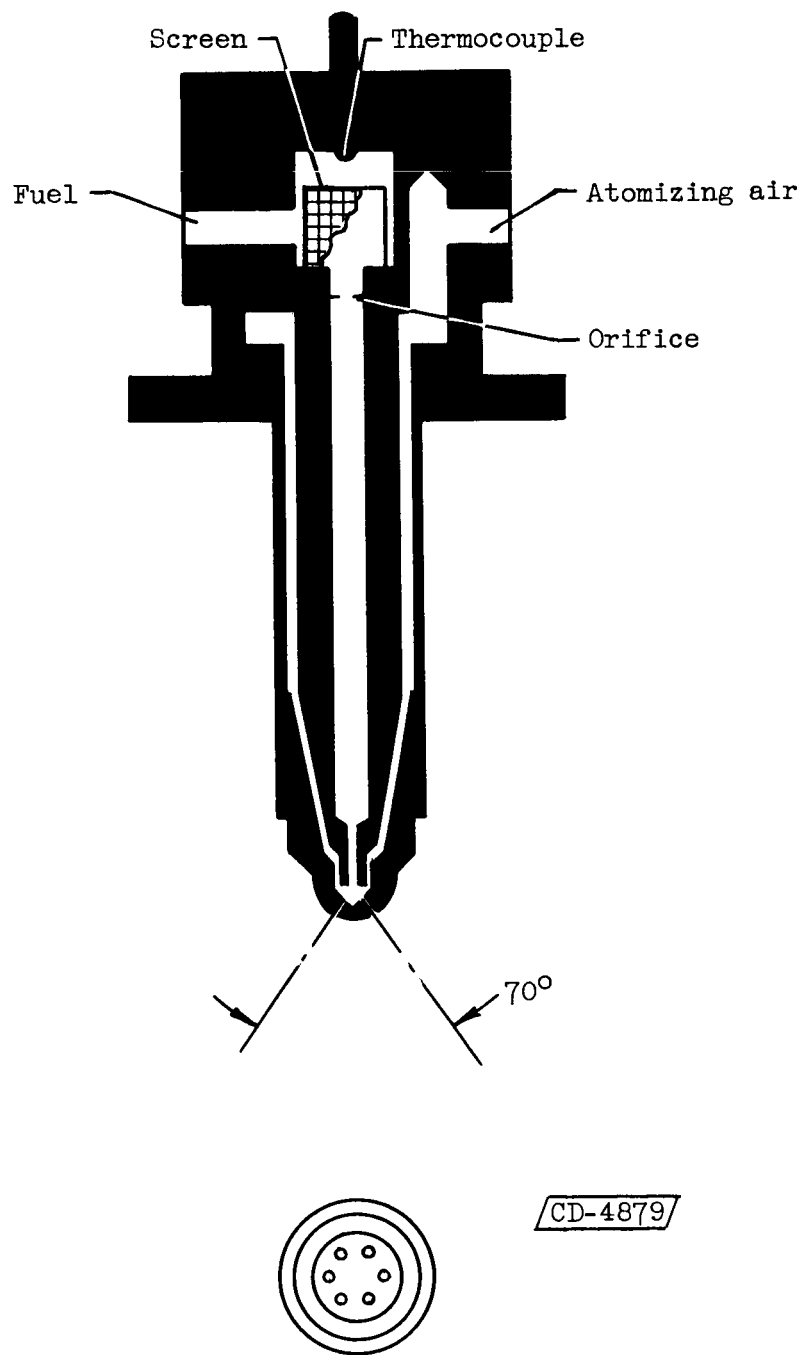


Figure 4. - Fuel-nozzle assembly.

CD-4879/

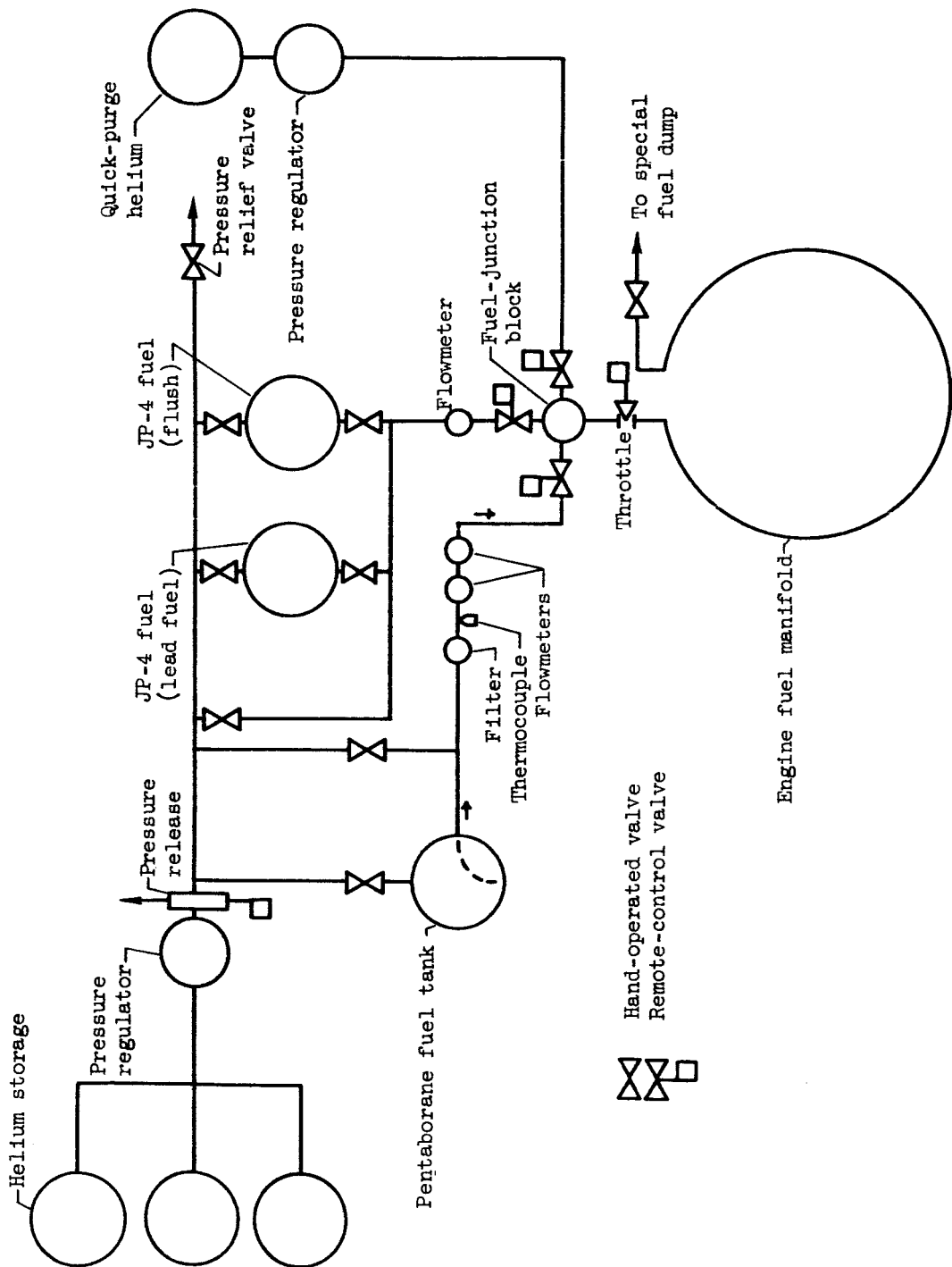
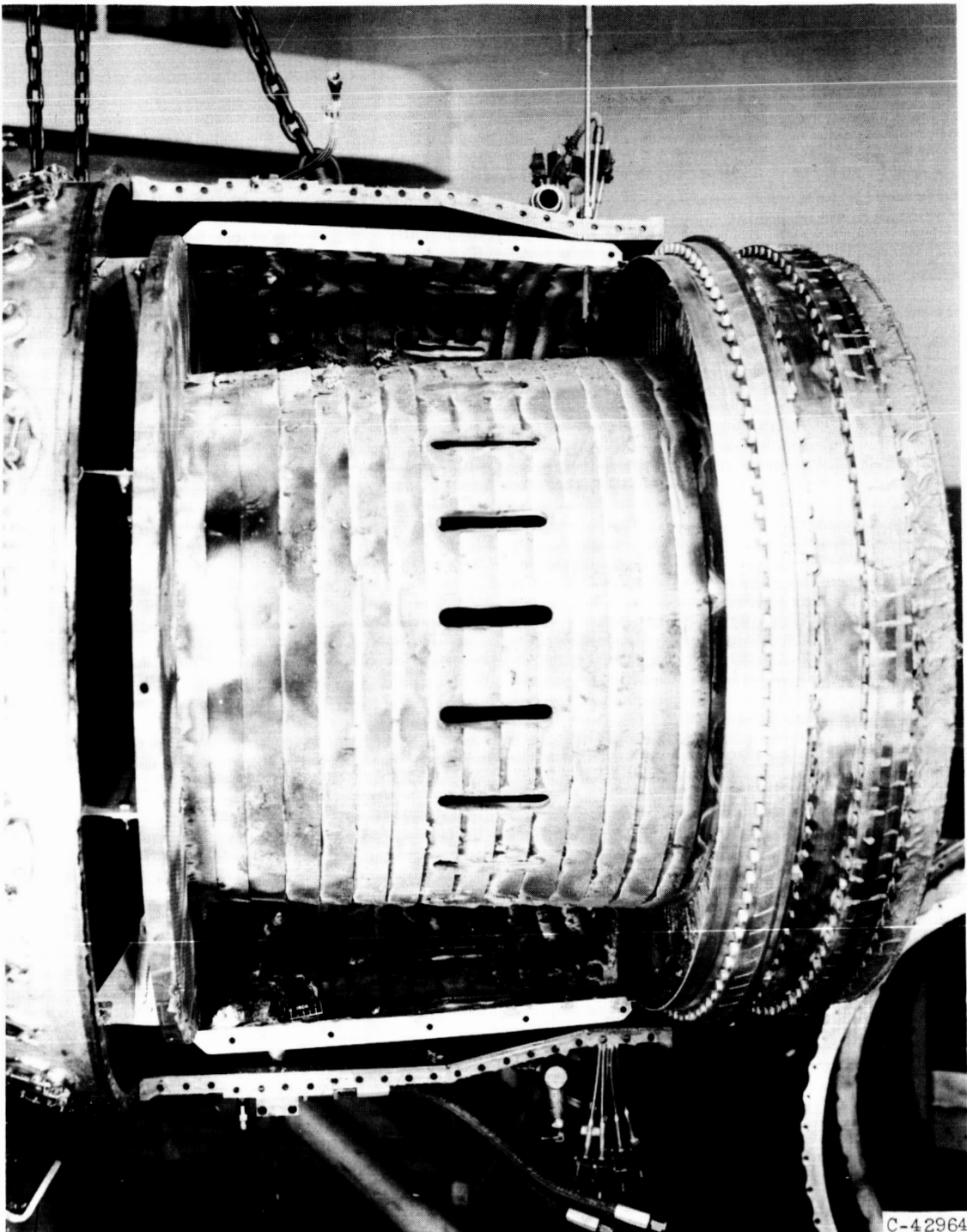


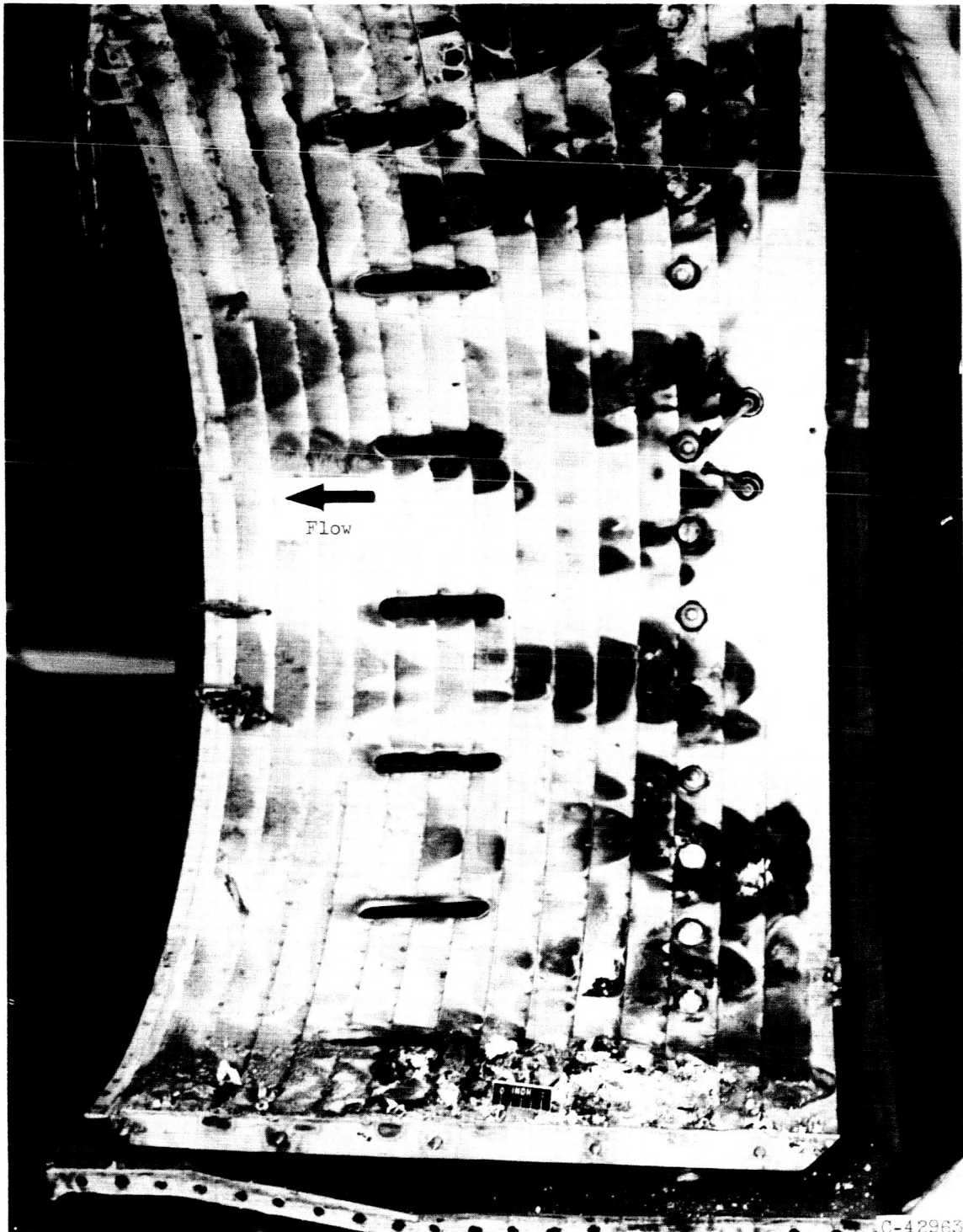
Figure 5. - Diagram of pentaborane fuel system.



C-42964

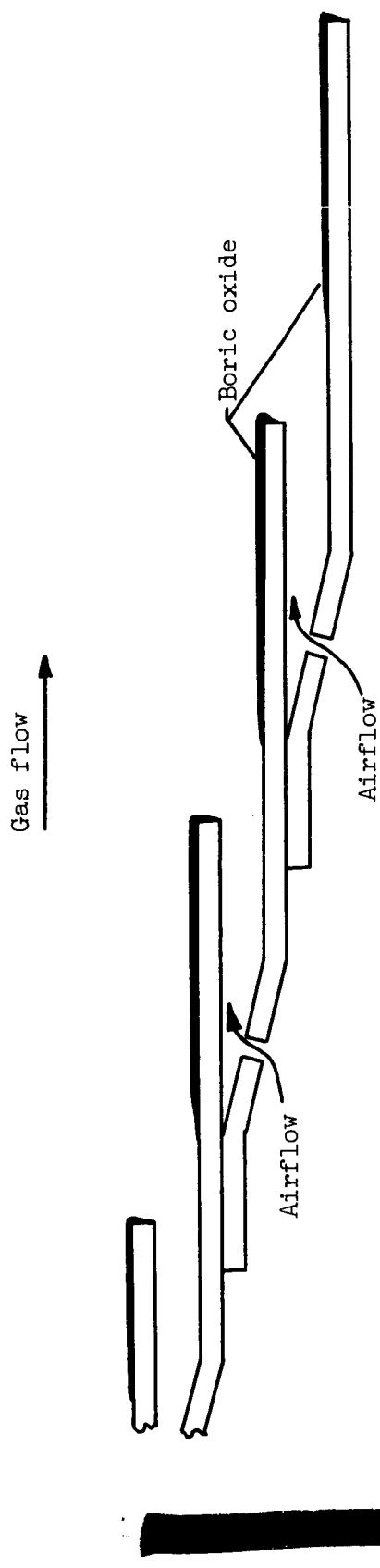
(a) Inner and outer combustor liners.

Figure 6. - Oxide deposition on combustor parts.



(b) Outer combustor liner.

Figure 6. - Continued. Oxide deposition on combustor parts.



(c) Schematic sketch of combustor wall showing location of boric oxide deposits.

Figure 6. - Concluded. Oxide deposition on combustor parts.



(a) First-stage stator, trailing edge.

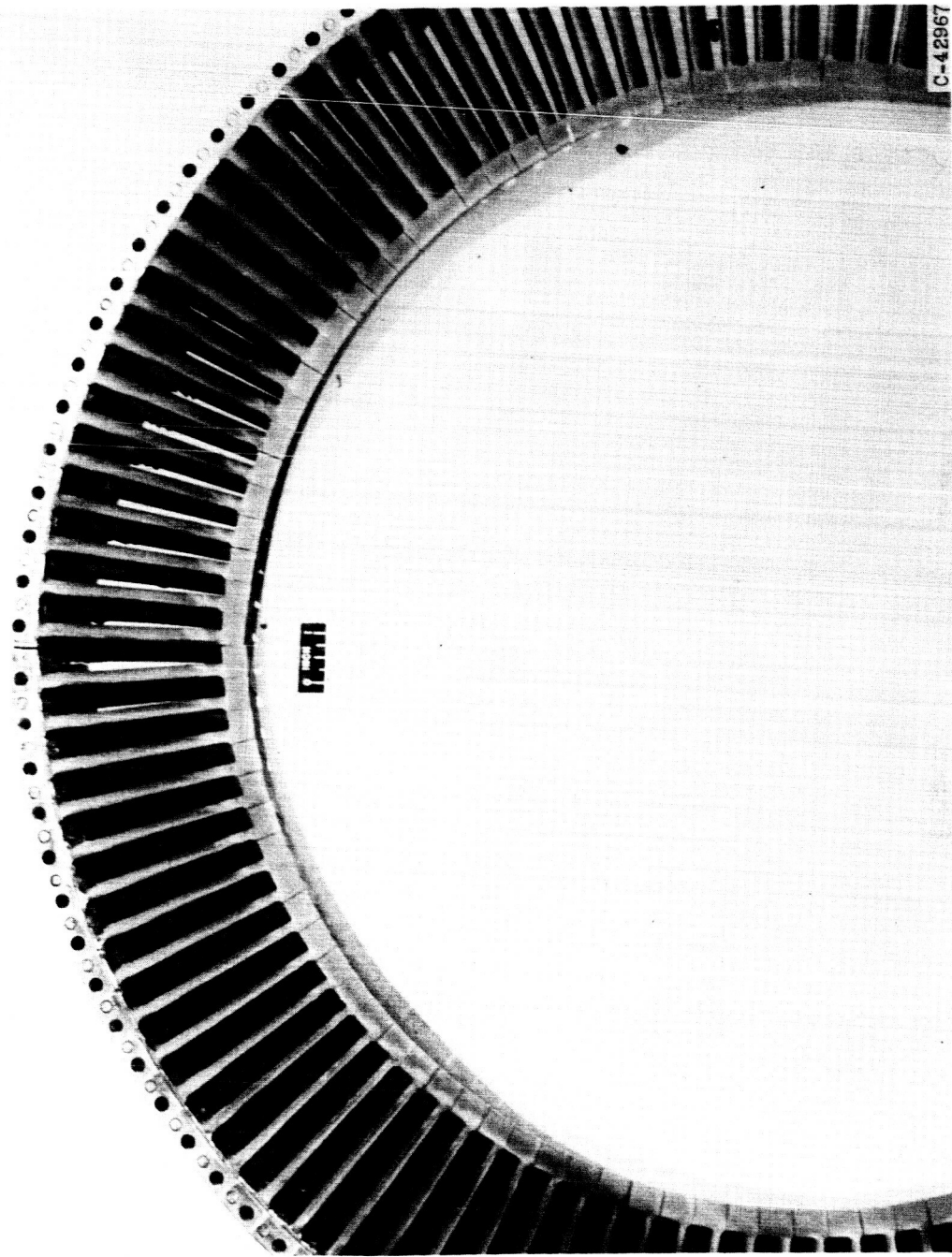
Figure 7. - Oxide deposition on turbine parts.

031200 1030

NACA RM E57C20



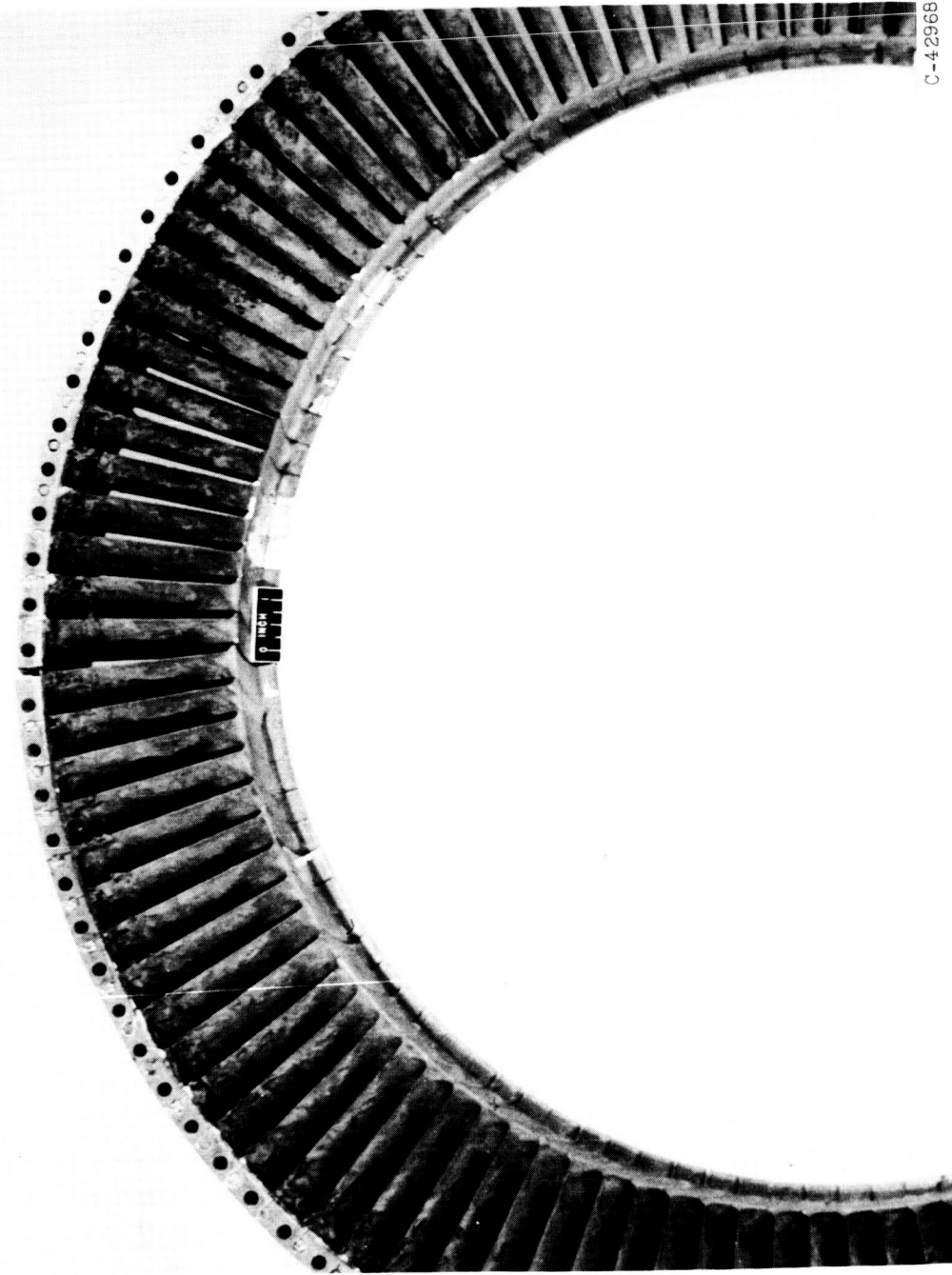
Figure 7. - Continued. Oxide deposition on turbine parts.  
(b) First-stage rotor.



(c) Second-stage stator, leading edge.  
Figure 7. - Continued. Oxide deposition on turbine parts.

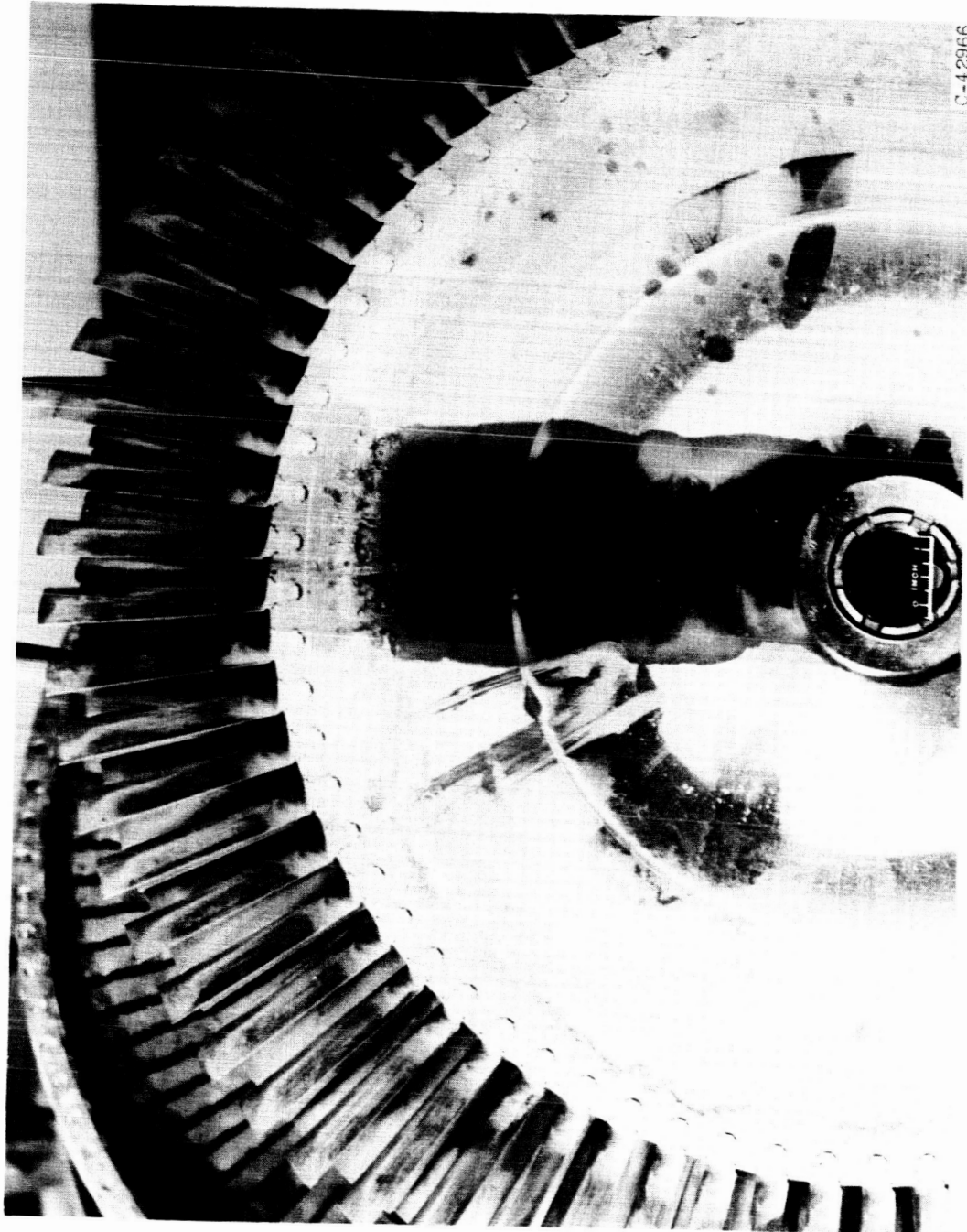
03030303030

NACA RM E57C20



(d) Second-stage stator, trailing edge.

Figure 7. - Continued. Oxide deposition on turbine parts.

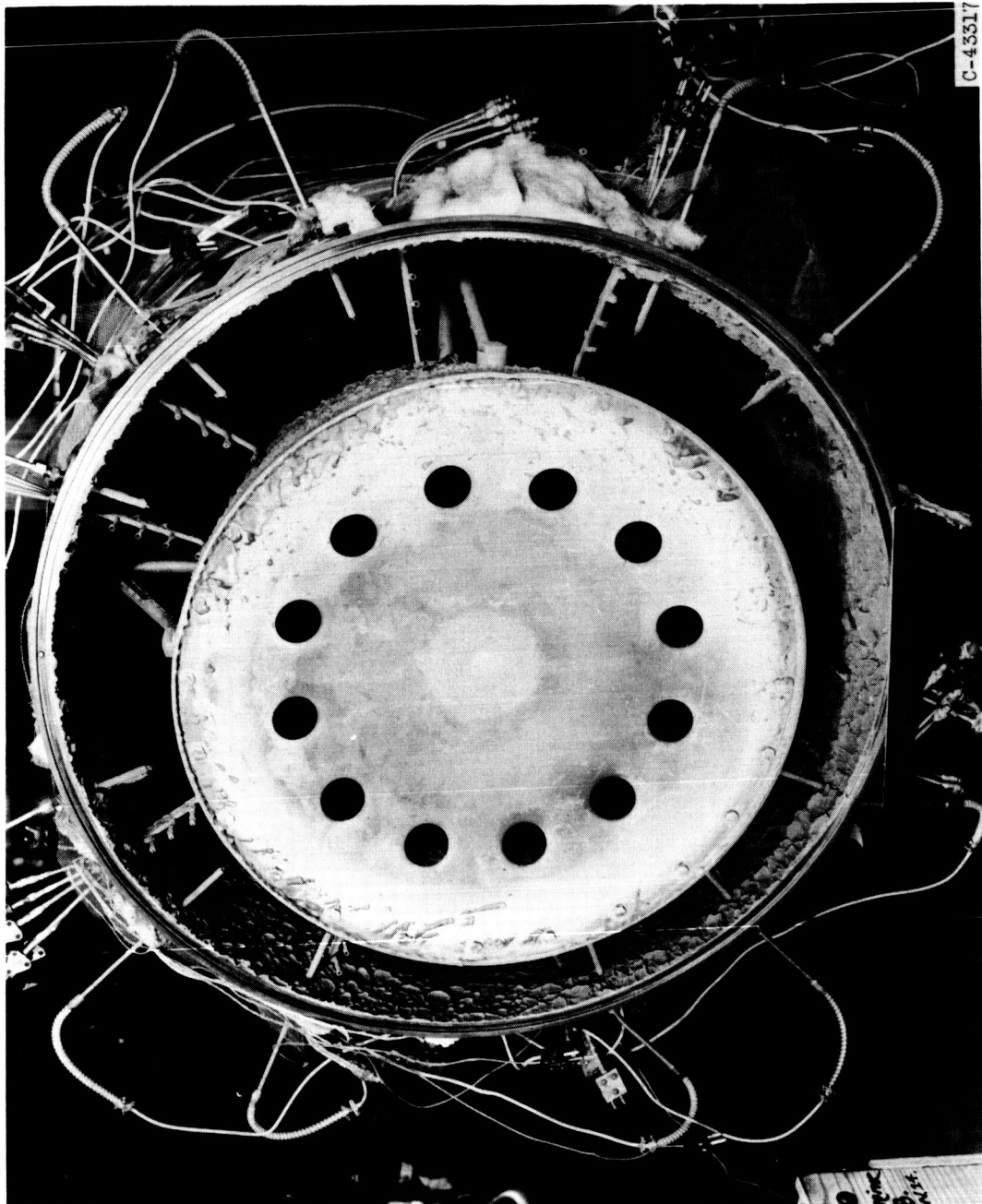
~~DECLASSIFIED~~

C-42966

(e) Second-stage rotor.

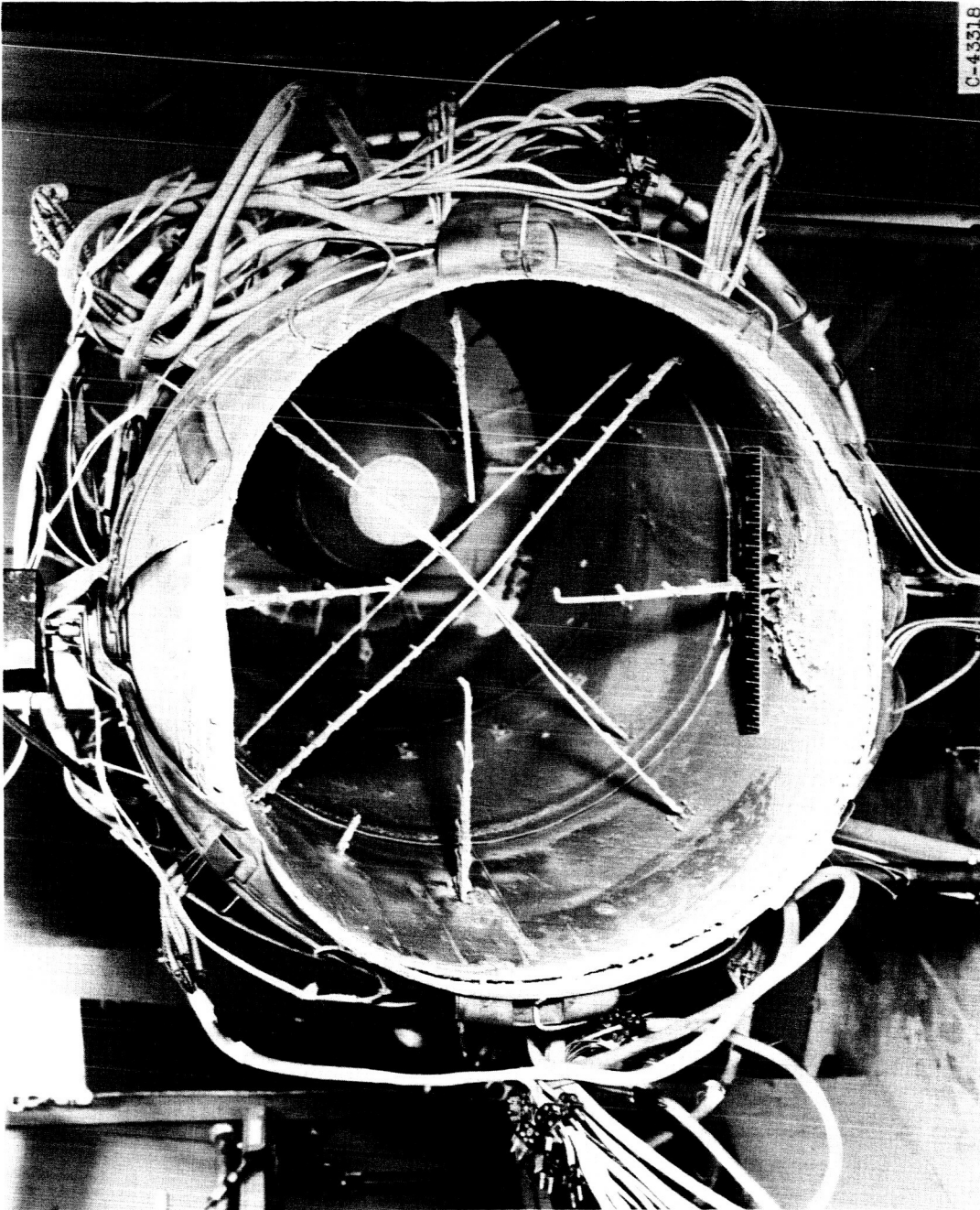
Figure 7. - Concluded. Oxide deposition on turbine parts.

03170201030



(a) Tailpipe diffuser.

Figure 8. - Oxide deposits on engine tailpipe diffuser, tailpipe, and exhaust nozzle.



(b) Engine tailpipe and exhaust nozzle.  
Figure 8. - Concluded. Oxide deposits on engine tailpipe diffuser, tailpipe, and exhaust nozzle.

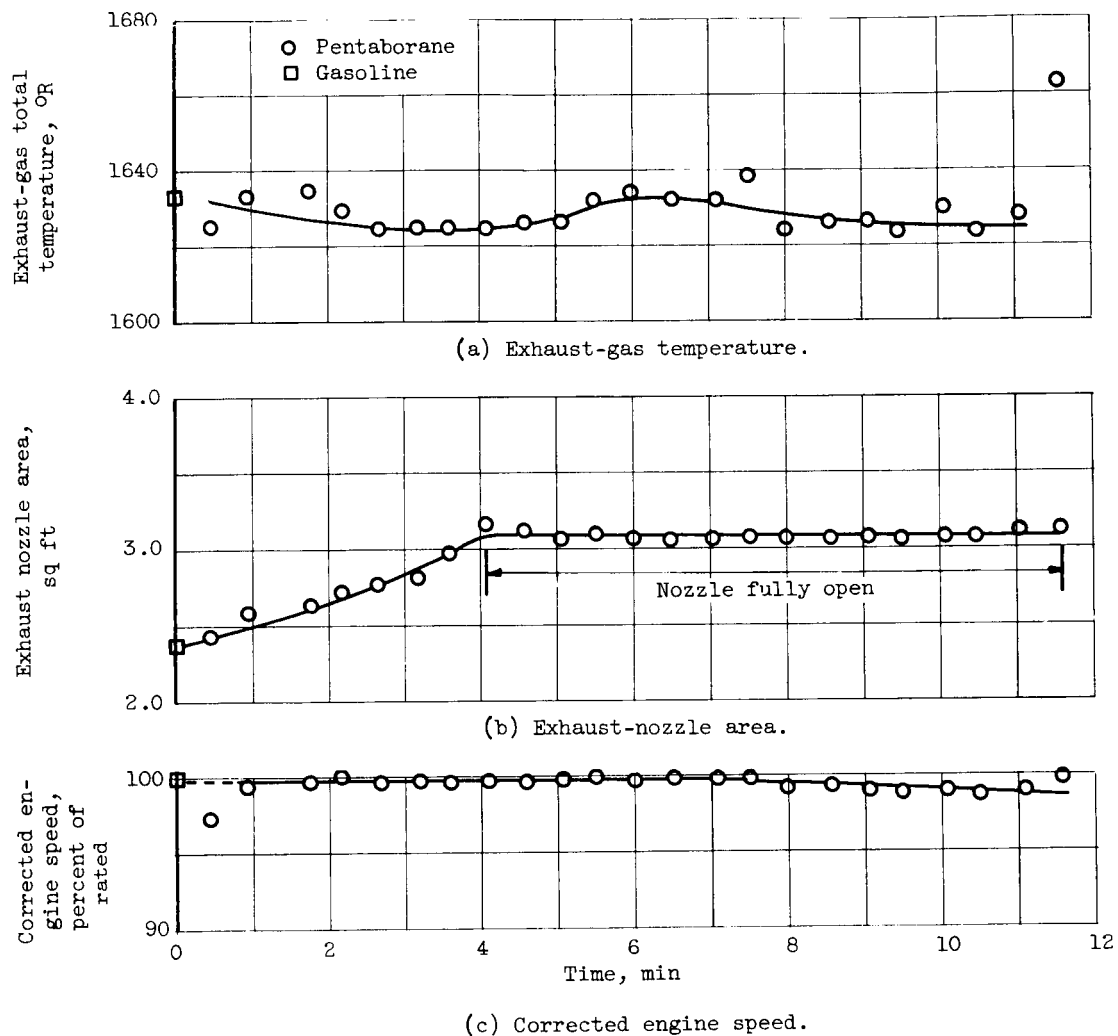


Figure 9. - Variation in exhaust-gas total temperature, exhaust-nozzle area, and corrected engine speed with time for operation with pentaborane.

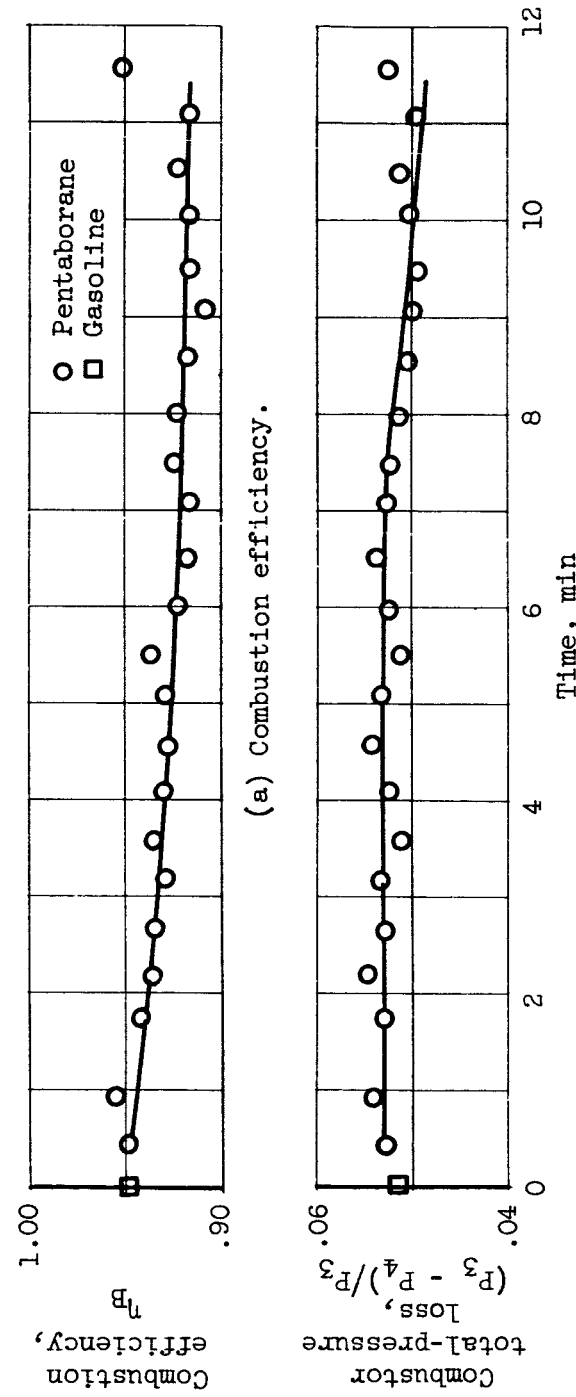


Figure 10. - Effect of operation with pentaborane fuel on combustor performance.

03100

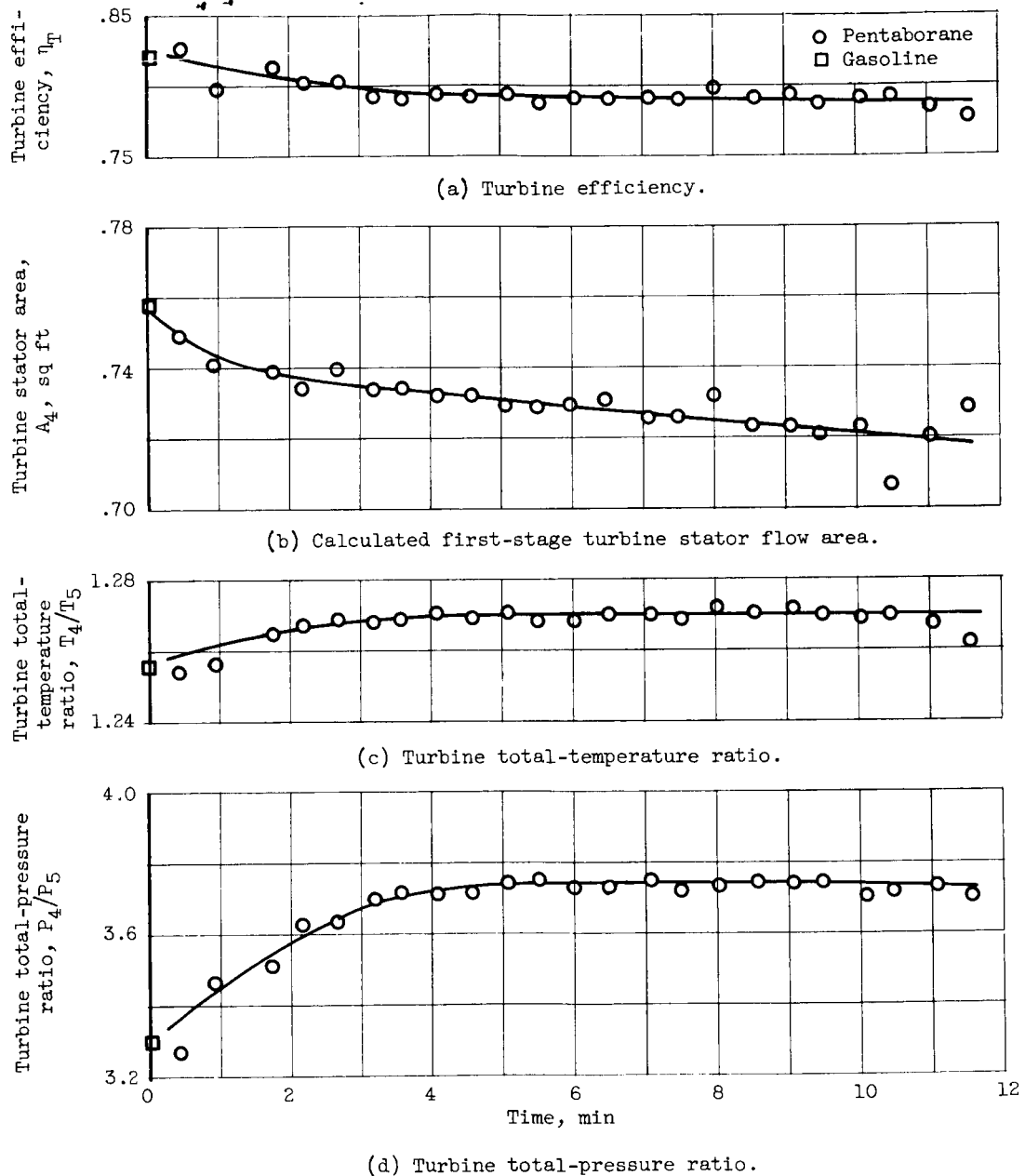


Figure 11. - Effect of operation with pentaborane fuel on turbine performance.

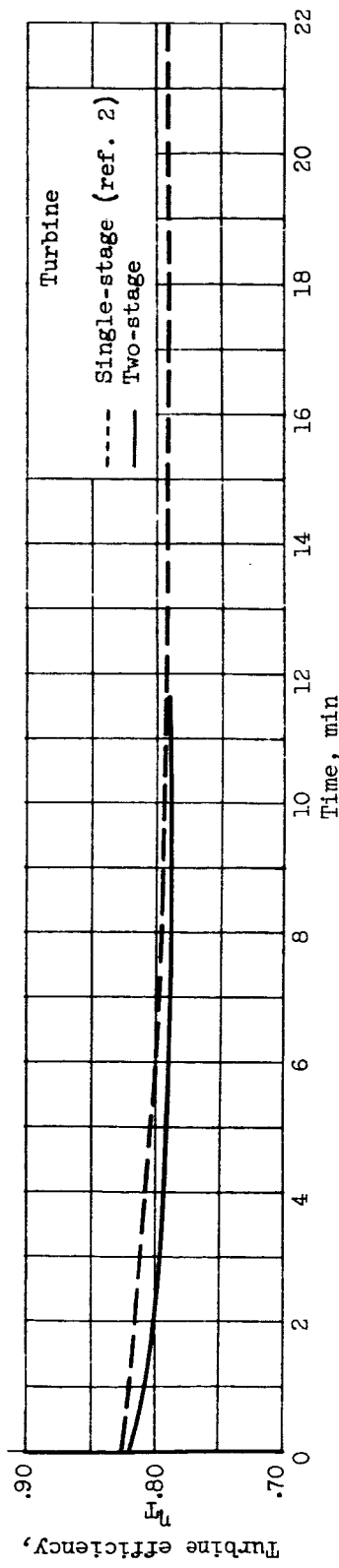


Figure 12. - Comparison of turbine efficiency for two-stage turbine with turbine efficiency obtained with single-stage turbine of reference 2.

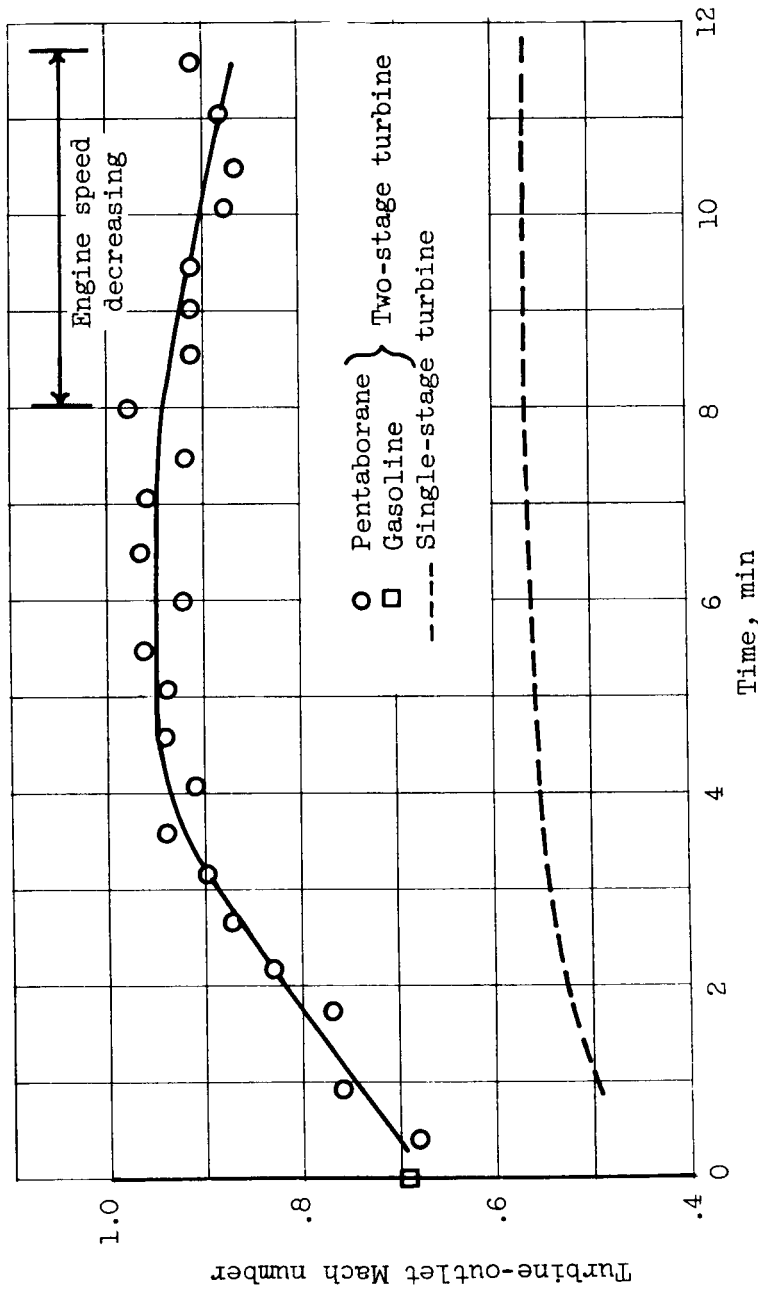
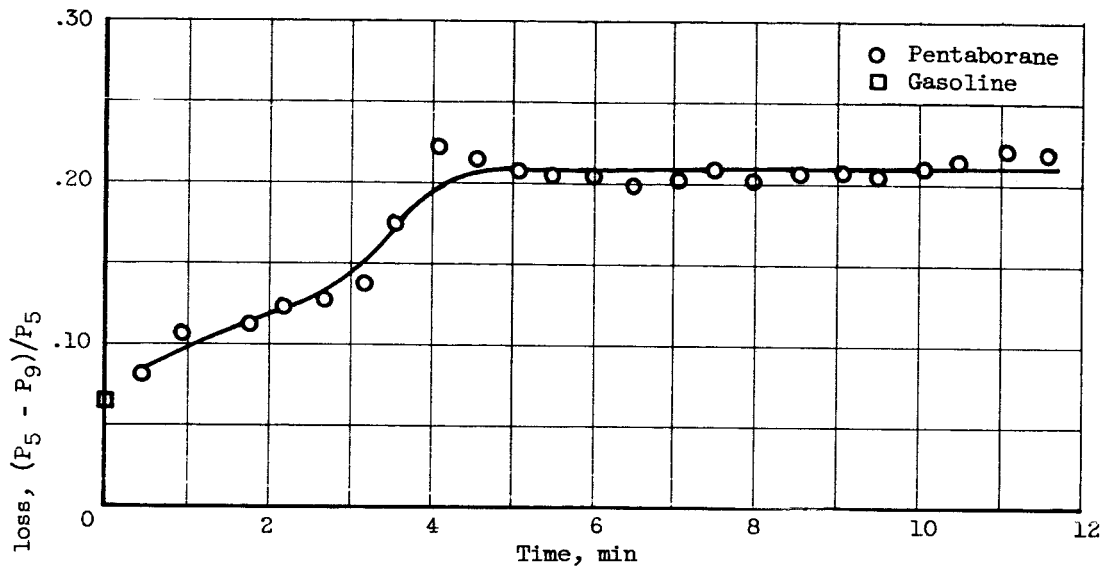
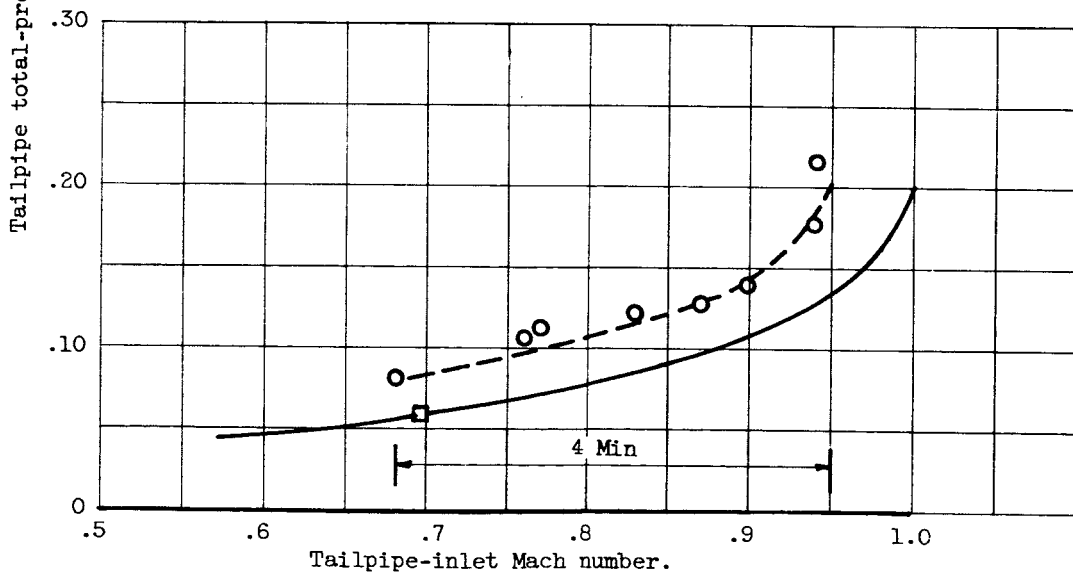


Figure 13. - Variation of turbine-outlet Mach number during operation with pentaborane fuel.

4384



(a) Effect of time.



(b) Effect of tailpipe-inlet Mach number.

Figure 14. - Effect of operation with pentaborane fuel on tailpipe performance.

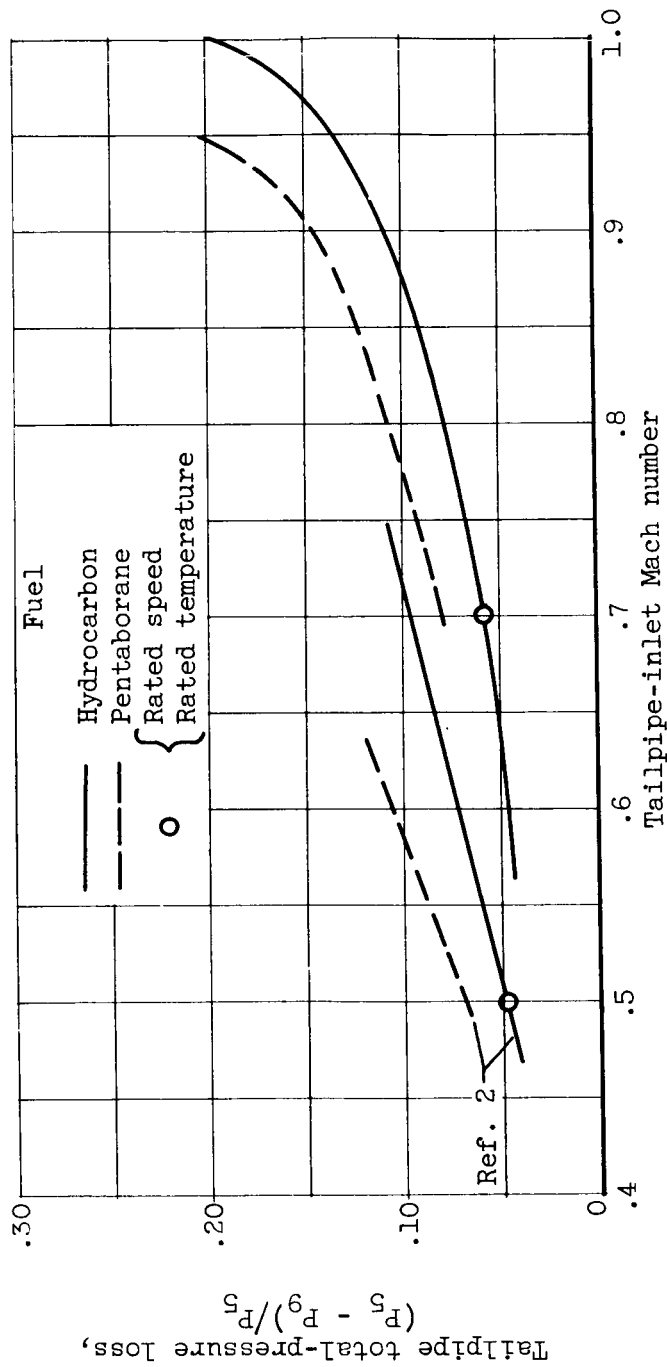


Figure 15. - Comparison of tailpipe total-pressure loss with loss encountered in reference 2.

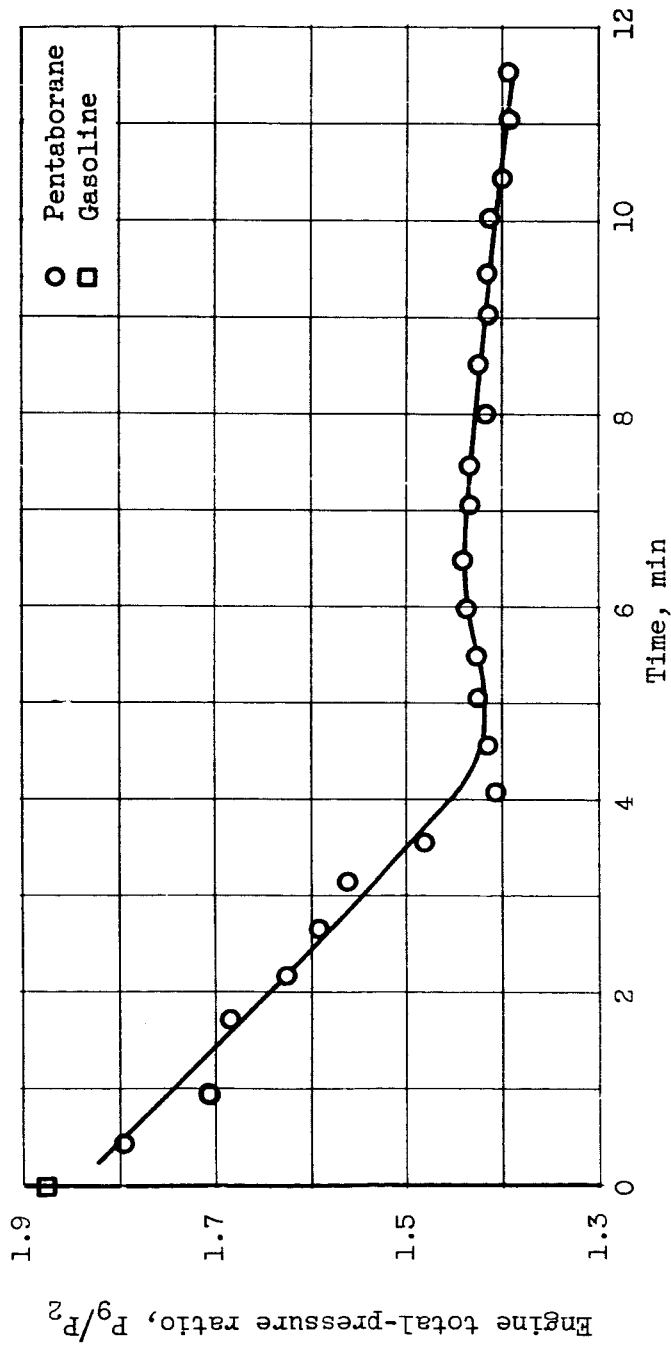


Figure 16. - Effect of operation with pentaborane fuel on engine total-pressure ratio.

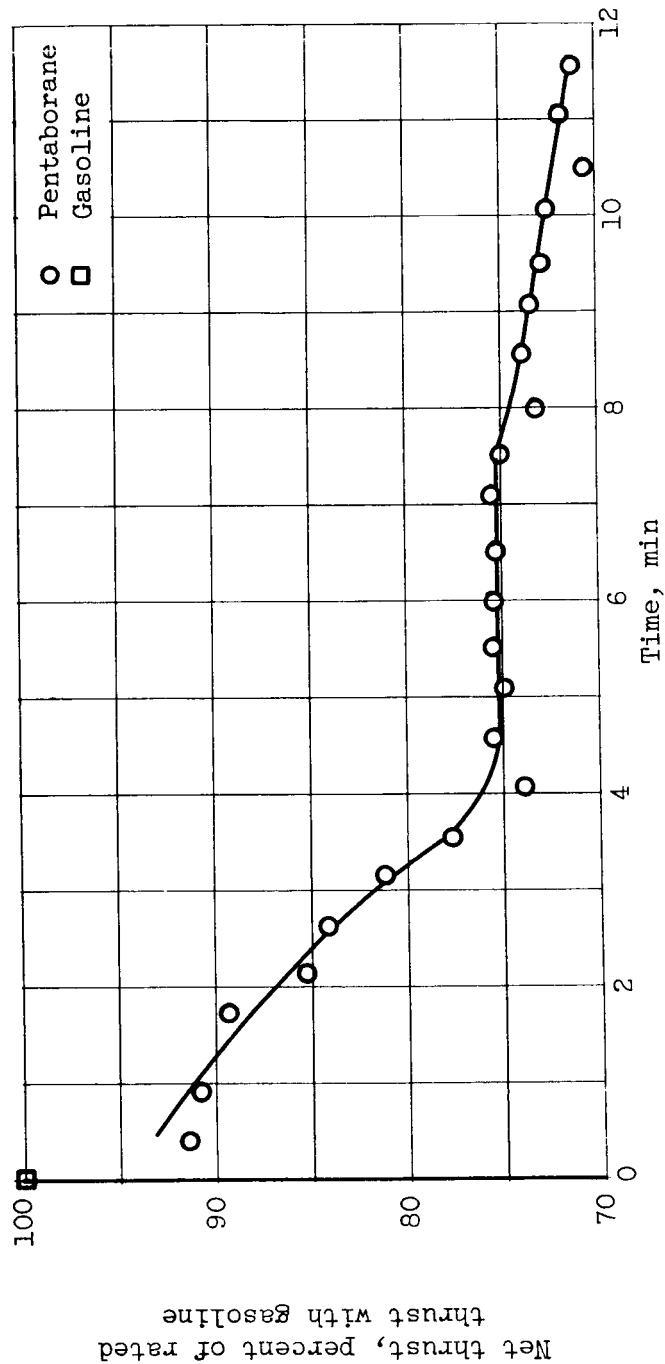


Figure 17. - Effect of operation with pentaborane fuel on net thrust.

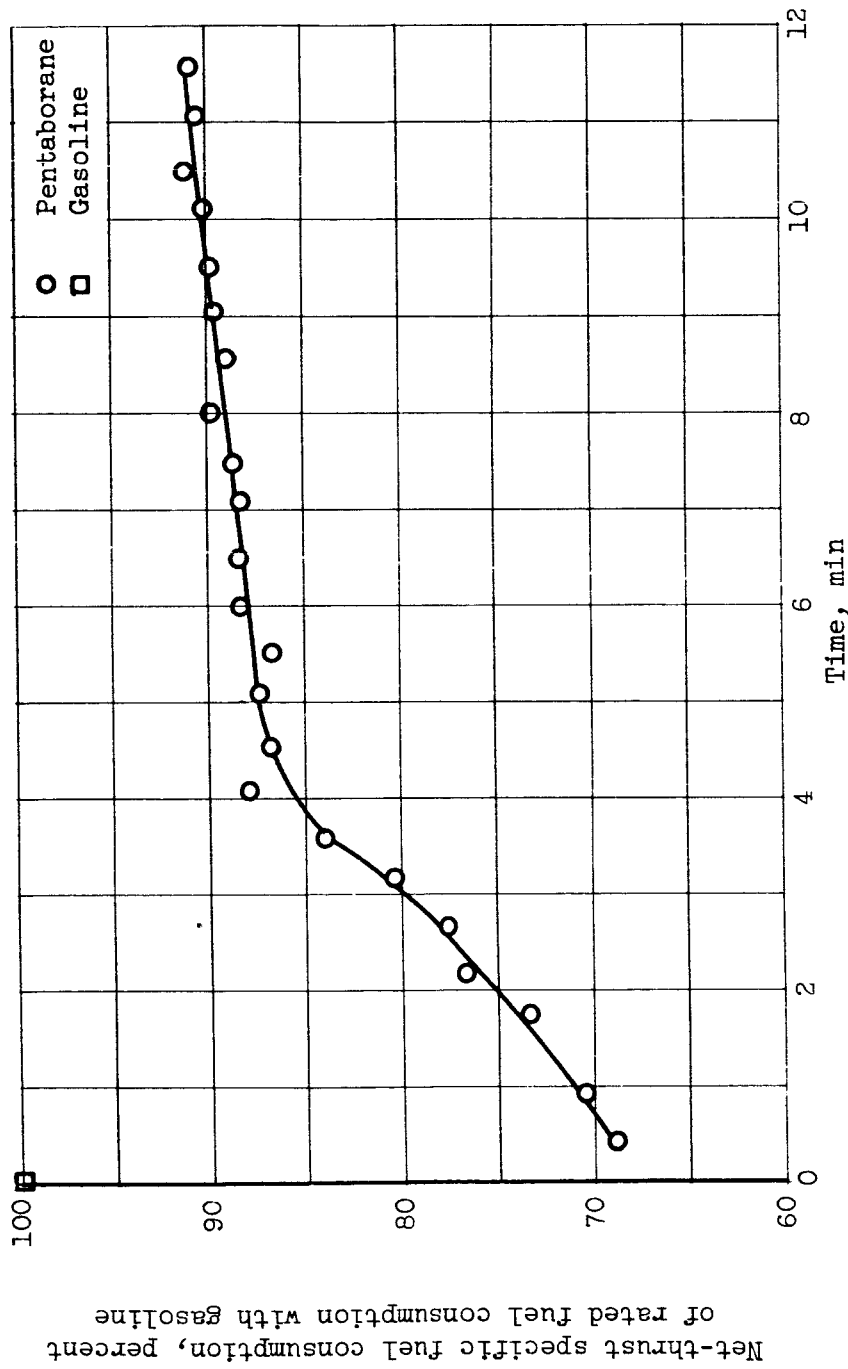


Figure 18. - Effect of operation with pentaborane fuel on net-thrust specific fuel consumption.

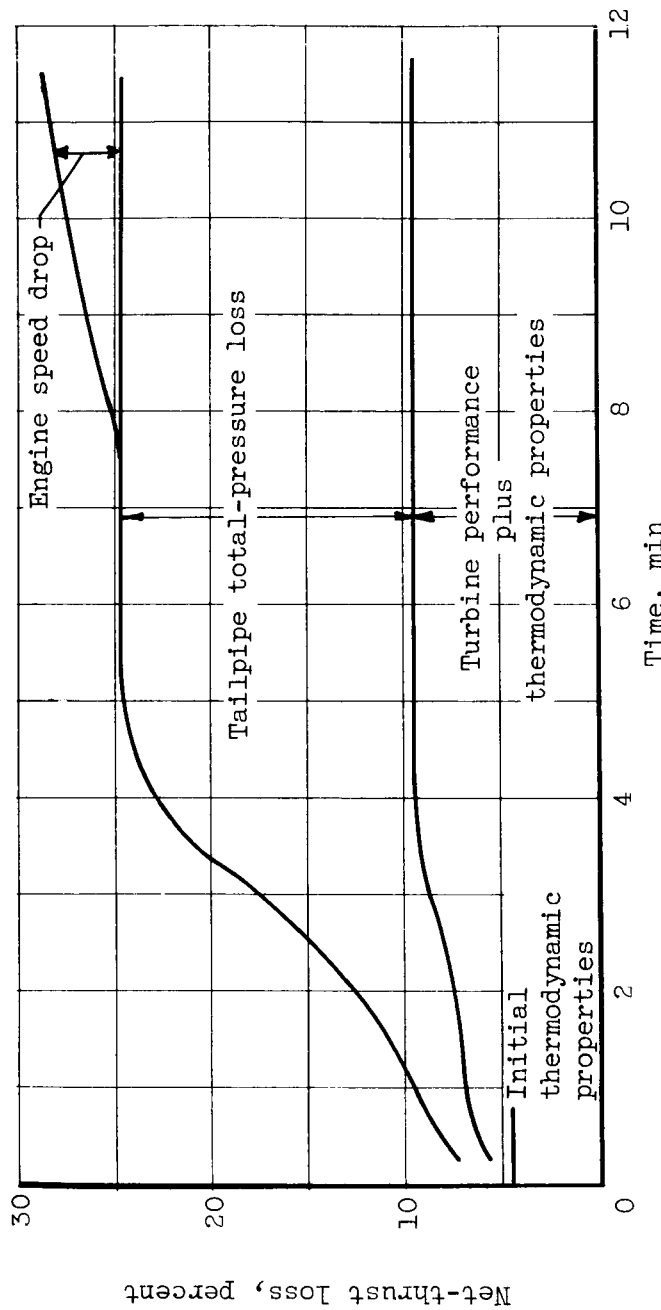


Figure 19. - Net-thrust losses with use of pentaborane fuel.